UNIVERSITÀ DEGLI STUDI DI PADOVA

Dipartimento di Fisica e Astronomia "Galileo Galilei"

Master Degree in Astrophysics and Cosmology

Final Dissertation

Habitability of planets in star clusters via interstellar lithopanspermia

Thesis supervisor:
Prof. Michela Mapelli
Thesis co-supervisors:
Prof. Simon Portegies Zwart
Dr. Veronica Saz Ulibarrena

Candidate:
Maria Francesca Cecchi

Academic Year 2021/22

To Zio Enzo

and to my Family

Abstract

We calculate the probability that a life-bearing planetary system in a young star cluster enriches another planetary system in the same cluster. This form of lithopanspermia has so far received little attention. We explore the possible cross fertilization of planetary systems by performing direct N-body simulations of star clusters in which we launch germinated asteroids from a selected sample of 0.9–1.1 $M_\odot$ main-sequence stars. We focus on star clusters which are consistent with the Sun's birth cluster ($\sim$ 2500 stars in a $\sim$ 1 pc virialized Plummer sphere). We calculate the dynamical evolution of the star cluster, while start launching asteroids after 100 Myr to 1 Gyr to study arrival time distribution of germinated-asteroid, therewith constraining the transport time from a life-bearing planetary system to uninhabited ones. The Galactic tidal field drives the cluster's dissolution on a time scale of a few hundred Myr. For younger clusters, the travel time for an asteroid to reach another star is smaller and the probability of reaching another star higher. We argue that the best moment to germinate multiple stars is as soon as life emerges on one of the cluster members. The asteroid travel time in this period is 10 Myr, which is sufficiently short for resilient extremophiles to survive the unfavorable interstellar conditions.

Contents

Chapter 1

Introduction

In the past decades, the long standing debate in the astrobiology community has lead to the widely accepted hypothesis of *panspermia*, which postulates that life can travel between planets and planetary systems.

The term *panspermia*, that comes from the Greek words $\pi\alpha\nu$ ('all') and $\sigma\pi\epsilon\rho\mu\alpha$ ('seed'), was firstly coined by the Greek philosopher Anaxagoras, who was an enthusiast of natural science and sought in the Universe the origin of life on our world.

We are intrigued by panspermia because, according to modern studies, the Earth was initially characterized by a sterile environment due to the high temperatures in the primordial phase. So far, there is still no evidence of the link between the inhospitable planet and the first forms of life, that appeared after $\sim$900 Myr from the birth of the Solar System. Indeed, the basic molecules at the origin of life should have required from millions to billions of years to forms complex structures such as the DNA. Therefore, they could have developed in other planetary systems and subsequently landed on our planet.

Moreover, it is possible that the Earth can be in turn the one responsible for the re-seeding of life in other planetary systems via asteroids.

In order for this to happen, it is necessary the presence of rock fragments that encase microorganisms, since the naked microscopic forms of life do not survive if exposed to UV radiation for more than minutes in the space environment, thus increasing the chances of viability of dormant microorganisms or DNA traces.

This thesis is a study on the origin of life on the Earth, emphasizing the evolution of the primordial organisms and focusing on their first evidence on our planet. This work will enlighten some of the gaps in the development of terrestrial life, as we can see in Chapter 2, that could be explained by introducing the concept of the lithopanspermia. The latter is explored in Chapter 3.

In particular, this mechanisms can be especially effective within a star cluster, where the stellar density is high, the relative velocities are low and thus the transfer of life is enhanced. The dynamics of a star cluster is described in Chapter 4.

We decided to perform a numerical simulation with the AMUSE environment, that is an open-source library that combines multiple codes from different astrophysical domains and that provides high quality performance (Chapter 5).

The method adopted for the analysis pursued in this work is presented in Chapter 6, where we explain the model for the star cluster that evolves in the potential well of the Milky Way, and the asteroids that travel within and beyond it.

Finally, Chapter 7 outlines the most important results given from the analysis of the simulations, leading to important implications for the theory of lithopanspermia.

In the Conclusions, you can find a summary of the results together with possible future developments.

Chapter 2

Origin of life

For many years the scientific debate on how life on our planet was born has involved an ever-increasing number of researchers, including several Nobel laureates for Medicine and Chemistry such as Harold Urey, Ilya Prigogine, Walter Gilbert, Christian De Duve and Francis Crick.

The experiments carried out so far have not led to a shared conclusion by all, but they have made it possible to shed light on numerous related problems to the mechanisms of life, such as those on the structure of nucleic acids and on functionality and peculiarities of biological proteins [13].

2.1 The life on the Earth

2.1.1 Simplest forms of life

Although most of the researchers disagree on the beginning, they share the same idea that the first and the simplest forms of life had to be linked to three types of **molecules**, capable of carrying out the following functions: the replicating, the catalytic and the insulating one from the environment. At the present time the first function is performed by **nucleic acids**, while the the second essentially from **proteins** and the last from **lipid molecules**. All these molecules aggregated together form structures (microspheres, liposomes, coacervates) that can generate duplicates of themselves but do not have the ability to transmit real information such as nucleic acids: only the latter have the function of coding and transmitting information.

Today the three types of molecules work simultaneously to allow the metabolism and reproduction of a cell and, in the case of lipid membranes, the protection of these processes from the external environment. Since many biological reactions are activated by **water**, the membranes can constitute a defense against the dispersion of the substances produced in a liquid environment. The origin of these three substances on Earth is therefore linked to problem of the origin of life [13].

2.1.2 The Miller's experiment

The first ideas about the birth of life supported by experiments date back to at least two centuries ago. For hundreds of years it was believed in the existence of a "spontaneous generation" of life, because observing stagnant water or organic substances left in the open air, like algae, fungi, molds or larvae, as if they were born out of nothing.

But already in the 1700s the Dutch Van Leeuwenhoek, inventor of the microscope, had observed and described those little shadows that he saw moving in the eyepiece of his instrument, the **bacteria**, proving that forms of life invisible to the naked eye exist. Following these studies, around 1862 Louis Pasteur conducted experiments which showed how in small enviromnets, **isolated from the air**, there was no spontaneous generation of molds or fungi, nor deterioration of food. He knew these microscopic life forms in the air were responsible for the contamination and reproduction of other microorganisms, and that preventing them from entering, the water would have remained sterile.

He was however far from conceiving life as generated and transmitted by molecules and considering metabolic processes as an effect of chemical reactions. The idea that the first forms of life were born from chemical reactions was developed only sixty years later, between 1920 and 1930, by the British John B.S. Haldane and the Soviet Aleksandr Ivanovich Oparin. Both speculated that life had spawned on the Earth from chemical processes that took place in an atmosphere rich in reducing substances (compounds containing hydrogen). This type of atmosphere is noticeably different from the current one, where oxygen molecules can sustain strong processes of oxidation. The **Oparin hypothesis** was experimentally tested in the 1950s by **Harold Urey** and his graduate student **Stanley Miller**, who tried to simulate in the laboratory the chemical composition of what was believed to be the primitive terrestrial atmosphere in the presence of oceans. They mixed in a bowl methane, hydrogen, ammonia and water vapor by subjecting the gas to electric discharges. In the experiments, the gaseous mixture had to look like to the **primitive atmosphere**, the water represented the **primordial oceans** and the electrical discharges any **atmospheric lightning**. Miller liquid is defined generally *primordial soup*.

Nevertheless, it can be said that the experiment was very approximate: none of the conditions have been calibrated with experimental data on the percentages of substances present on the primordial Earth, because of the few information then known on the first epochs of ours planet nor of the outermost planets of the Solar System. After several days of producing vapors and electric discharges, the aqueous solution extracted from the container included numerous organic compounds. Numerous similar experiments, conducted in subsequent years with variants of the original mixture, produced similar results.

Despite numerous controversies, the value of this experiment is supported by the fact that it can describe a plausible mechanism for the emergence of prebiotic substances. The synthesized amino acids have a high probability of withstanding harsh environmental conditions and the passage of time, thus they can be reused to form even more complex molecules. Substances that do not present high stability would not be very useful in the first processes of formation of the life, unless they are present in very large quantities.

In more recent experiments, Miller has managed to produce almost all 20 amino

acids that enter in cellular metabolism. In the reducing atmosphere[1] the generation of nitrogenous bases is also possible, but in this case not all of them resist for a long time, for example pyrimidines. The synthesis of amino acids and pyrimidines is possible in a wide range of conditions, as they were found in carbonaceous chondrites, born in space.

The experiments on the production of prebiotic substances in the local conditions of a planet only confirm the wide range of possibilities that exist in their synthesis. Miller's experiment has finally led to understand that **prebiotic compounds** require, for their formation, the **presence of reducing gases**. Indeed, in the following years it was attempted the synthesis of organic compounds in oxidizing or neutral environmental conditions with the same mechanism (water, energy and gas mixtures). These experiments showed that it is not easy to produce these substances except in small quantities and with a stability lower than that of synthesis in a reducing atmosphere [13].

For what concerns the **nitrogenous bases**, it is known that some similar molecules have been found in carbonaceous chondrites. To understand and simulate the mechanisms of their formation, the **formamide**, a molecule spread in interstellar space, it was mixed with meteorite dust of various types and irradiated by beams of high-energy protons, mimicking cosmic rays. This experiment, carried out in the laboratory simulating the space conditions, produced a wide variety of important prebiotic compounds such as amino acids, carboxylic acids, nitrogenous bases, sugars and, in particular, four nucleosides: cytidine, uridine, adenosine and thymidine. This implies that on the primordial Earth, in addition to the formation of amino acids, bases of nucleic acids could have come through **cosmic dust or even impacts**, leading to the trigger of the first living processes [13].

2.1.3 The Last Universal Common Ancestor

The greatest difficulty is not finding molecules capable of reproducing and interacting with the environment, possibly shielding themselves with layers of organic substances, as bacteria do today. Instead, it seems to be the acquisition of a very selective structure, with precise rules, which must have been transmitted unchanged over time up to the current species.

Taking this genetic tree back in time, they all seem to have a common ancestor, called *unique precursor* or **LUCA**, which is the acronym of *Last Universal Common Ancestor*. It allows us to explain the particularities of carbon-based terrestrial life, that can be synthesized by the following scheme:

- only 5 nitrogenous bases (A, T, C, G, U)
- only 20 amino acids

[1] A reducing atmosphere is an atmospheric condition in which oxidation is prevented by removal of oxygen and other oxidizing gases or vapours, and which may contain actively reducing gases such as hydrogen, carbon monoxide, and gases such as hydrogen sulfide that would be oxidized by any present oxygen. [1]

- pentose sugars only (rings of 5 carbon atoms)
- only amino acids L and only sugars D (chirality)
- bonds with phosphorus and sulfur, rarer elements than C, N, O, H
- the genetic code

All the studies carried out so far have shown that there is no physics-chemical reason for these particularities to be established. They could be just a coincidence: by chance on our planet a cell that we call LUCA and that possessed these specific properties began to reproduce, thus generating over the billions of years the variety of species we know today.

This hypothesis is reasonable and apparently without consequences. However, it contains in itself an important insight: if chirality and the current selection of amino acids are only a legacy of our precursor, perhaps precursors have been able to develop in **other different environments**, based on carbon, but with amino acids or sugars or chiralities different from those of terrestrial life. This idea, which is attractive from a philosophical point of view, suggests us not to be too rigid in our search for life in space, even if it is not known whether it is possible to develop a life with molecules other than ours [13].

2.1.4 Ratio $C^{13}/\ C^{12}$

In order to understand how life formed on Earth, the first important goal is to find out what reactions can generate a molecule or micro-structure capable of replicating and interacting with the environment through a form of metabolism similar to those of terrestrial life forms.

However, the problem becomes more complicated if the most important methods to infer the times for life development are based on geology and paleontology. The age of a rock can be determined through radiometric methods. If living beings are made of carbon atoms, in their metabolism they mainly fix only one of the two stable isotopes that exist in nature: **carbon 12 (C^{12})** composed of 6 protons and 6 neutrons, and the **isotope (C^{13})**, that has an extra neutron in the nucleus and is therefore a heavier atom. In nature, physical and chemical processes that take place at lower energy are privileged.

In this case, life forms make more use of the lighter isotope, C^{12}, and when animals and plants die, they release the amount absorbed during their life into the soil. The soil is thus enriched with C^{12}. At the origin of the Earth, the C^{13} / C^{12} ratio was the "cosmic" one ($\sim$ 50/1000), determined by the nuclear fusion processes inside the stars. Once processes are born that segregate the lighter isotope, on the ground this ratio is lowered (i.e. the amount of C^{12} in the denominator increases) until it reaches the "biological" one in living plants (11/1000).

Reversing the reasoning, if the isotope ratio of carbon is measured, it can be established whether a soil (or for instance a meteorite that contains carbon) has been influenced by life forms. This effect is expressed with the **variation of the C^{13} / C^{12} ratio**, referred to a standard that marks an arbitrary zero point. This **standard**, in 1957, was

identified with the isotope ratio measured in the calcite of the fossil of a Cretaceous mollusk, Belemnitella americana, found in the Pee Dee formation of South Carolina (USA). For this reason the standard was called PDB (Pee Dee Belemnite). Subsequently, the International Atomic Energy Agency (IAEA) in Vienna has redefined the standard, which is known as **VPDB** (Vienna Pee Dee Belemnite). The ratio R = C^{13} / C^{12} in the case of the sample fossil is RVPDB = 11.237 % and is naturally very distant from that present in the interstellar material. By measuring R in an object, each variation from RVPDB is calculated through the formula:

$$\delta C^{13}[\%] = 1000x(R/R_{VPDB} - 1) \tag{2.1}$$

In sea water there is δ C^{13} close to 0, in grass growing in arid areas it reaches -13 % and in leaves up to -27 %, as listed in Table 2.1. Since δ C^{13} decreases with time due to the metabolism of living beings, by measuring the isotope ratios of the carbon of increasingly ancient rocks, it is possible to establish the approximate epoch in which life forms on Earth began to metabolize carbon. Another factor for the lowering of δ C^{13} to values of $\sim$ -15 is the presence of kerogen, a mixture of substances of biological origin found in sediments, which under pressure and over a very long time can form bitumen, oil, natural gas, graphite.

Source	δ C^{13} [%]
1.5 $M_\odot$ stars (theoretical value)	3000 - 3900
Carbonaceous chondrites	25 - 75
Standard VPDB	0
CO3 marine	0
Soil CO2	-5
Atmospheric CO2	-9
Grass in arid area	-13
Martian meteorite ALH84001	-15
Marine organisms and plants	-16
Petrified wood, charcoal	-24
Maximum value in plants (rice, potatoes)	-33
Methane in anaerobic zones	-60

Table 2.1: Approximate values of δ C^{13} (in thousandths) in stars, meteorites, on the earth's surface and in living organisms. Extraterrestrial objects are indicated in italics.

However, the isotope segregation mechanism also occurs in the case of **evaporation**: the lighter isotope evaporates more easily, and the reservoir of material from which it comes is enriched with the heavier isotope. On Earth this happens for the oxygen, hydrogen and carbon contained in water (H_20) and methane (CH_4). For instance, the methane oxidation process mainly involves the lighter molecules, that are converted into carbon dioxide. If this gas is reduced again, it will have a low quantity of C^{13} and its presence will lower the value of δ C^{13}, **mimicking what happens in biological processes**. On another planet, for example Mars, rocks with high values of δ C^{13} could

therefore derive from "fossil" life forms or from methane deriving from non-biological processes.

Unfortunately, plate tectonics alters and reshapes most continents on Earth and it is difficult to measure traces of life on extremely ancient rocks. However the oldest datable rocks have an age of 3.96 Gyr and the oldest known crystals (zircons) have an age of 4.3 Gyr [13].

2.1.5 Earliest traces of carbon

Furthermore, we can infer the date of the formation of our planet at around 4.6 Gyr from the studies on the most ancient meteorites. We know that Earth and the nearby Moon have suffered an **intense bombardment** of planetesimals and asteroids. The violent impacts of these rocky bodies on our soil pierce the crust and make the basalts of the mantle come out. Therefore these regions appear younger than the rest of the crust.

Lunar rocks brought back to Earth by Apollo astronauts show an age of 3.85 Gyr for the Mare Imbrium, a huge impact crater 1300 km in diameter, and $\sim$ 3.5 Gyr for the Oceanus Procellarum. The age of other lunar terrains from which it was not possible to bring back fragments of rocks is established by counting the **number of craters** present per surface unit, grouped by diameter. It is based on the idea that the more a terrain has been exposed to the outside, the more impacts it has received and therefore it must have more craters. This method is not very accurate also because it is difficult to apply to small regions. By applying this procedure, it is deduced that impacts strong enough to create craters such as Copernicus (93 km in diameter) or Tycho (102 km) occurred more recently, respectively 800 and 109 million years ago. Craters of a few hundred kilometers in diameter are produced by the impact of rocky objects of a few kilometers, which release to the ground an energy equivalent to that of an explosion of $\sim$ 100,000 Megatons, capable of burning everything for hundreds of km.

We can think that the Earth, subject to the Heavy Bombardment phase, was a **very inhospitable** place for the life forms that were being born there. Impacts with objects larger than 100 km would have even been sterilizing for the whole planet. We can therefore suppose that, as long as the initial bombardment of planetesimals was massive, up to 3.5 billion years ago, when the lunar seas were formed, the Earth's surface environment must have been hot and subject to abrupt changes in physical conditions [13].

On Earth, the oldest sedimentary rocks have been discovered in the Isua Greenstone Belt, West Greenland, dating back to 3.8 Gyr ago. These rocks, partially metamorphosed over the past billions of years, derive from the deposition of sediments carried by the wind and water on the seabed or oceans. If this were the case, expanses of water must have already been present 3.95 Gyr ago. In these regions the sediments show a carbon content in the form of graphite and kerogen with $\delta\ C^{13}$ values from -13 to -28 %, while the carbonates present have values of $\sim$ -3 [38].

Even higher values were measured in younger sedimentary rocks, in Pilbara (Australia), with an age of 3.5 - 3.4 Gyr and with $\delta\ C^{13} \sim$ -26 %, and in the island of Akilia, Greenland, with age of 3.83 Gyr and $\delta\ C^{13} = -37\%$. These values indicate that the earliest traces of organic carbon enrichment can be dated to **before 3.95 Gyr ago**, when the Earth was born very hot, hundreds of degrees, and gradually cools, bombarded

by enormous impacts while the gases contained within it reach the surface through the volcanoes. The water vapor forms the rains that carry sands into the oceans, where what today are sedimentary rocks begin to form. Based on radiometric dating, this occurs at $\sim$ 3.95 Gyr in the past. If together with the formation of oceans, created by the boiling and sterile water of volcanoes, there are already forms of life that have produced the value of $\delta\ C^{13}$ measured today, it may mean that **life developed immediately**, as soon as there were right conditions for its development [13].

2.1.6 Fossil bacteria

It takes hundreds of millions of years to go from chemical traces of life to bacteria. Microstructures interpreted as fossil bacteria have been found in Pilbara, Australia, in rocks of 3.47 and 3.45 Gyr, and in the Barberton Mountains, South Africa, in rocks between 3.1 and 3.2 Gyr. These fossils represent remnants of single cells and groups, arranged in filaments or grouped, with 11 different species of organisms classified on the basis of the shape and structures of the filaments themselves. Some of them resemble today's cyanobacteria. There are also carbonaceous filamentous structures $\sim$ 2 µm wide and tens to a few hundred µm long, similar to those of modern filamentous bacteria. The $\delta\ C^{13}$ value ranges from -30 to -42.4% with respect to the PDB.

In addition to these microscopic structures, there are others with a spherical or filamentous shape similar to fossils, found within stratified sediments. These stratifications are produced by bacteria, which capture marine sediment particles in regions affected by the tide or in shallow water, enclosing them in interwoven lamina or filament structures. When the cells die, the sedimentary particles remain cemented to form a thin sheet of flint (SiO_2). Each new layer that forms with new bacteria can trap other particles, producing dome-shaped layered structures called **stromatolites**.

On the other hand, if the plates are dragged by currents, rolling on the seabed, spherical stratified structures are formed, called **oncolites**. Since both derive from biological activity, they are generically called **organogenic-sedimentary structures**. Stromatolites can still form today, due to colonies of cyanobacteria, with a lower frequency than in the past. Some Australian stromatolites and oncolites have an age between 3.2 and 3.5 Gyr and are another fossil evidence of the presence of life in an age of more than 3 Gyr. If these stromatolites were produced, like the current ones, by cyanobacteria, we must think that oxygen began to be produced biologically already at that time [13].

2.1.7 Great Oxidation Event

However, it is necessary to go up to $\sim$ 2 billion years ago to find the first signs of a strong oxidation of the atmosphere, probably as a result of the spread of **photosynthesis** on a planetary level. This strong oxygenation of the atmosphere is known as the **Great Oxidation Event**, or Oxygen Catastrophe.

The anoxic seas and the ground begin to absorb oxygen already at 2.5 Gyr, while the ozone layer is formed between 1.9 Gyr and 850 Myr, from excess oxygen. After this time it begins to accumulate in the atmosphere. The geological evidence of the presence of oxygen is manifested first with siliceous rocks that contain reddish layers of iron oxide,

indicative of the release of small amounts of oxygen into the atmosphere or hydrosphere. These layers may have formed in primitive, anoxic oceans, where iron must have existed in the form Fe_2 (ferrous), soluble and dissolved in seawater. The appearance of oxygen in superficial waters due to the presence of bacteria may have transformed it into Fe_3 (ferric), producing hydrated iron oxides, insoluble and capable of precipitating on the seabed, accumulating with silica. Siliceous rocks with bands of iron oxides appear on all present continents and are referred to as BIF (Banded Iron Formations). They have an age between 3.2 and 2 Gyr and disappear in sediments younger than$\sim$ 2 billion years.

After this period, deposits of reddish, yellow or brown rocks appear, called Red Beds and formed by layers of limonite, trivalent iron oxide (Fe_2O_3).

The emergence of oxygen-producing organisms may have held back the synthesis of new molecules and amino acids, but it has not extinguished the anaerobic microorganisms. They have populated niches far from the surface, such as the ocean floor or the subsoil, where we still find them today.

Similarly, the appearance of photosynthesis did not stop bacterial chemo-synthesis: in the same epochs, in addition to photosynthetic bacteria, other prokaryotes operated different types of metabolisms, including nitrogen fixation. The availability of atmospheric oxygen must have favored the birth of the breathing process, which allowed the use of oxygen that would otherwise be dangerous for many bacteria [13].

2.1.8 An explosive phenomenon

In conclusion of this Section we must note a problem that emerges from the recent dating of the first traces of life and the age of terrestrial rocks. The Earth is born very hot, hundreds of degrees, and progressively cools while the gases contained within it reach the surface through the volcanoes. The formation of a solid crust can be traced back to 4.3 Gyr. The water vapor of the volcanoes forms the rains that carry sands into the oceans, where what today are the sedimentary rocks begin to form. Based on radiometric dating, this occurs at $\sim$ 3.95 Gyr in the past. Based on the age of the rocks of the lunar seas, we can hypothesize that the Heavy Bombardment lasted at least up to 3.5 Gyr, creating an inhospitable surface environment, with strong variations in temperature. Indeed destructive impacts have also continued to this day, but with less frequency. On the basis of the estimates of the formation models of the Solar System, the frequency of impacts had however decreased by 100 million times from 4.3 to 3.5 Gyr, while remaining $\sim$ 10 times greater than the current one. But based on measured isotope ratios, life must already be present on our planet around 3.95 Gyr. And referring to fossils, bacteria could have existed on our planet in epochs of 3.46 Gyr (Pilbara) or 3.5 Gyr (Australian stromatolites). But how could bacteria or life forms exist on an Earth still under the effect of the devastation of gigantic impacts, capable of forming lava lakes on the Moon, with a certainly similar effect on our planetary crust?

If together with the formation of oceans, created by the boiling and sterile water of volcanoes, at 3.95 Gyr there are already forms of life that have produced the value of δC^{13} measured today, it may mean that life is an **explosive phenomenon** , which arises as soon as the right conditions for its development are in place, even during the Heavy Bombardment. However, on the Earth's surface there was an ocean or anoxic pools of

water in contact with an atmosphere full of carbon dioxide, such as the one that Venus and Mars still present today.

Then only special environments, rich in hydrogen, that could generate the chemistry necessary for a primordial soup similar to that reproduced in the experiments of Urey and Miller could be the areas around **volcanoes**, both in air or submarines.

However, even admitting to locate the birthplaces of primordial terrestrial life, the time available for all the chemical processes that gave rise to the first forms of life is not measured in billions of years, but in hundreds of millions or less. If we then think of the 3.46 Gyr fossils, a molecule capable of reproducing itself and having its own metabolism is not enough to generate such large and complex structures. To have a fossil of a bacterium it is necessary that a whole sequence of molecules have already formed and collaborate together: nucleic acids for reproduction, proteins for metabolism and lipids for cell walls, traces of which can be found in the fossils. All this has been achieved in less than half a billion years from the birth of life.

How could carbon enrichment have been achieved as soon as the oceans were born and under the meteorite bombardment? We can imagine three possibilities: catalysis, birth in regions isolated from the outside or panspermia.

In the first possibility there should have been a very effective mechanism that guided the synthesis of the first molecules in such a way that, once the optimal conditions for the birth of life occurred, it could form very quickly. There should therefore have been a **physical or chemical catalyst**, such as pyrites or other substances. However, there is currently no evidence to firmly believe that this strong catalyst exists.

The second hypothesis is that life could have formed in the depths of the ground or of the oceans, where even the Heavy Bombardment could have a minor effect on more stable environmental conditions. In this case, the energy for biochemical synthesis would not come from solar radiation, but from **volcanic thermal energy** or **gas chemosynthesis**. We will discuss about it in the Sec. 2.1.9.

A third possibility is part of the general idea that life, being based on chemical elements spread throughout the galaxy, could have been born in space in the dust clouds with a synthesis lasting billions of years and then arrived on Earth in the form of granules of dust or carried by comets. We will discuss about it in Chapter 3. [13]

2.1.9 Isolated regions

In this hypothesis, the biological mechanisms would have been born on Earth but far from the surface exposed to the Heavy Bombardment and therefore to unstable conditions. Only later, when surface conditions would allow it, would life forms colonize the surface of the oceans and land emerged.

This hypothesis is linked to the idea that life was born completely on Earth, supposing that the first forms of life were generated in particular environments in which reducing gases are abundant, such as hot pools heated by volcanoes (hydrothermal springs). If we stick to Miller's hypothesis, which sees light and electrical discharges as the energy sources for the synthesis of prebiotic substances in a reducing atmosphere, we can imagine the biological origins in warm and shallow waters with chemical reactions stimulated by solar UV rays, not yet shielded by the atmospheric ozone layer. In the vicinity of terrestrial

volcanoes, gaseous emissions include, in addition to carbon dioxide, hydrogen sulphide and methane, also other substances containing hydrogen. Phosphorus, sulfur and nitrogen are also more abundant than the rest of the planet and can contribute to the formation of more complex substances.

In these areas, for example in the hydrothermal springs at Vulcano, in the Aeolian Islands, there are today microorganisms that can live at temperatures up to 114 ^oC. Other heat-loving **hyperthermophilic bacteria** develop at similar temperatures: Thermococcus, Pyrococcus, Hypertermus, Staphylothermus are found in environments up to 105 ^oC; Pyrodictium and Methanopyrus multiply between 110 and 130 ^oC.

From a genetic point of view, hyperthermophiles can be considered the oldest among existing bacteria. They are classified among the Archea and many use sulfur for their metabolism (sulphobacteria), producing methane (methanogens). Some sulphobacteria found near volcanoes can be both aerobic (thus they use atmospheric oxygen) and anaerobic.

We must expect that the first forms of life could have been born in extreme conditions of temperature, pressure and acidity, very different from the current ones, and that they therefore belong to a category of bacteria called **extremophiles**. Current extremophilic bacteria can live in areas with pH from 1.4 (very acidic) to 13.5 (very alkaline), with temperatures ranging between 130 ^oC (in volcanic regions) and -15 ^oC (in the frost in the Siberian permafrost), in water free of salts, but also up to 300% saturated with sodium chloride.

Terrestrial bacteria can remain **dormant** inside porous desert rocks, thus defended by harmful UV rays from the Sun, but are activated in the presence of water. They can remain frozen for millions of years in permafrost or included in marine sediments. Aerobic bacteria extracted from the 101-million-year-old marine sediments of the South Pacific have been successfully cultured in the laboratory. Extremophilic bacteria suitable for living in environments with very high pressures have been found in oil fields and in deep aquifer deposits. If life originated around volcanoes, it could have synthesized various hydrocarbons and organic acids, including all amino acids, from volcanic gases, with the catalytic contribution of metals, using heat rather than light or electrical discharges as a source of energy.

Nevertheless, in the air environment, high-temperature amino acids could be unstable. According to more recent studies, it is not the aerial hydrothermal springs that we must look at as the cradles of life, but the **submarine** ones. On the ocean floor, where the magma that escapes from the crust forms chains of volcanoes (ocean ridges), there are regions where volcanic gas, rich in metals, sulfur and hydrogen, feeds extremophilic chemosynthetic bacteria that once they allow life to marine animals in symbiosis with them. These isolated communities congregate around volcanic vents, called **black smokers**. The hot synthesis of amino acids alongside underwater volcanoes would allow the new molecules to move by convection and arrive in a very short time in waters with a lower temperature, where they would be stable [13].

2.2 Life in the Solar System

If life forms have also developed on Earth in environments with extreme physical and chemical conditions, these conditions are also present in other places in the Solar System. In recent years, an intense exploration activity of the planets and major satellites has been developed through the sending of automatic probes that explore them from orbit (orbiter) or that land on the ground (lander), exploring it with mobile robots (rover) . Some of these probes have tools for the chemical analysis of the atmosphere and soil and can provide us with important information on the planetary environment. In some cases, the instruments carried were specifically designed to search for extraterrestrial life forms.

Taking into account the wide range of environmental conditions in which extremophiles live, We can analyze the main possible planetary hosts for the primordial forms of life.

Mercury is too hot and too small to hold a biologically significant atmosphere. The **Moon** is also very small and unable to retain an atmosphere. Their surface is covered with craters, evidence of the Heavy Bombardment, and the substances present are often dissociated by high-energy solar radiation (UV, X). There is no surface water and volcanism was short lived. The same desolate picture is offered by many rocky satellites such as those of Uranus and asteroids. Their surface is cratered and with no atmosphere.

Venus is a very hot planet due to an imposing greenhouse effect, but which can still reserve surprises in the subsoil or in the high and colder clouds (see Sec.2.2.1).

Mars presents extremely interesting conditions, see Sec. 2.2.2.

On their journey to the outer Solar System, several space probes flew over the satellites of the outer planets and explored Pluto: around Jupiter the Pioneer and Voyager probes, Galileo and Juno, Saturn the Cassini probe, Uranus and Neptune the Voyager 2 probe and a Pluto the New Horizons. Many satellites are cratered and without atmosphere, while others like **Io**, a satellite of Jupiter, have active volcanoes fed by a huge tide, created by Jupiter on one side and by Europa and Ganymede on the other, which discharges its energy by heating the satellite. Due to the tides, the rocky surface of Io rises to 100 m. Its average temperature is 130 K ($-143\ ^oC$), but the numerous active volcanoes and the volcanic calderas present can reach temperatures of 1500 K. The tenuous atmosphere composed of sulphurous gases creates very particular environmental conditions compared to those of other regions of the Solar System. There are no hypotheses in favor of a possible presence of life on Io.

More promising are the other large satellites of Jupiter, **Europa** and **Ganymede**, and of Saturn, **Titan** and **Enceladus**. Covered by an icy crust that is several kilometers thick, they seem to guard an underground ocean hidden under the ice.

On **Triton**, Neptune's satellite, jets of nitrogen and dark dust, probably carbonaceous, have been observed. On **Pluto** a vast heart-shaped plain seems to hide a sea below.

Unfortunately, apart from the Galileo and Cassini missions that orbited Jupiter and Saturn for years, the missions that studied Uranus, Neptune and Pluto were limited to a close passage to the planet-satellite system and then lost in deep space. Anything interesting that has been observed cannot be deepened until a future mission with a journey of several years [13].

2.2.1 Venus

Venus has a mass and structure similar to that of the Earth, but the physical conditions on its surface are extremely different, due to the presence of a huge greenhouse effect. Since its formation 4.5 billion years ago, the volcanoes of Venus have produced greenhouse gases by discharging them into the atmosphere. If these gases are not altered by chemical processes and their components do not enter the rocks, they contribute to increasing the global temperature. Thus over billions of years its surface temperature has risen up to the current 465 ^oC, almost constant from the equator to the poles. This type of greenhouse effect is called **avalanche effect** because, once an imbalance threshold has been established and reached, it can only increase without any natural phenomenon being able to stop it.

As the emission of gas accumulates, the atmospheric pressure also increases. On Venus, it reached a value of 9.5 MPa on the ground, as in the seabed at almost 900 m of depth. For this reason it is believed that the surface of the planet is now **too hot** to host any form of life based on carbon or chemical reactions similar to ours. Furthermore, sulfur dioxide, SO_2, emitted by volcanoes combines with water vapor and hydrogen to form sulfuric acid, H_2SO_4, which is present in clouds and falls to the ground like a **corrosive** drizzle.

However, in 2020 radio observations revealed in the atmosphere of Venus along with many other molecular bands of known compounds, a single absorption line at 266.9 GHz, which was interpreted as due to phosphine (PH_3). This molecule undergoes a rapid degradation both by **photolysis** (dissociation due to the UV radiation of the Sun), and by **oxidation** due to the sulfuric acid of the clouds and in general through reactions of the O, H, and OH radicals, which transform it into PH_2 and other compounds. Although the intensity of the line was later corrected by electronic fluctuations in the signal, according to observers its presence is too high to think of an inorganic production with the mechanisms known on Earth, such as volcanic emissions and photolysis of phosphoric acid (H_3PO_4).

Phosphine has already been found in the atmospheres of Jupiter and Saturn, rich in reduced gases containing hydrogen, that is produced by the phosphates present in the clouds struck by lightning. It was identified on Titan and being a soluble substance in methane, which forms its lakes, and can be produced and re-emitted by non-biological mechanisms present on that planet. On Earth, however, it is formed in great quantities by bacteria in oxygen-free environments, such as those of animal organic residues. This process is the only one that could explain the abundance observed on Venus. But the detection of a single line of phosphine, among other things often observed in interstellar gas, in the midst of the numerous lines of SO_2 and CN molecules that could lead to a misinterpretation, has created a certain skepticism among radio astronomers, waiting of new data and confirmations.

If the phosphine were created from molecules of **biological origin**, it could be possible that life also appeared on Venus at the same time as Earth, 650 million years after its formation. If Venus had liquid water and a rotation period of a few hours, it could have harbored life forms for a period of a few billion years. However today Venus has a rotation period of 244 Earth days, longer than its year, of 225 days. Moreover, the

planets presents a retrograde rotation, that could be due to a huge impact, similar to that between proto-Earth and Theia, in the period of the Heavy Bombardment. The slowing down exposes it to prolonged solar radiation with accumulation of heat; this mechanism and the catastrophic event may have changed the surface of the planet, favoring the accumulation of volcanic gases and making it **inhospitable**.

The hypothetical Venusian life forms may have taken refuge in the **subsoil**, where the temperature decreases for tens of meters and where there may still be aquifers. Nevertheless the phosphine begins to decompose at 375 ^oC and therefore, even if it were generated by life forms now hidden in its subsoil, it could not cross the very dense layers of Venus, 100 degrees warmer, and be revealed at the top of the clouds.

As an alternative, Venusian life forms transported billions of years ago to high altitudes and took refuge there may have survived, suspended in the **clouds**. On Earth, clouds develop in the troposphere, the lowest layer of the atmosphere that reaches an altitude of 12 km. More than 1800 bacterial species have been found in the troposphere. Microorganisms and spores have been discovered up to 77 km above sea level, in the stratosphere, transported upwards by storms and monsoons, along with dust and water droplets. On Venus the troposphere reaches much higher, at 60 km. At that altitude, the pressure is similar to that of the Earth, 100 KPa and temperatures range from 0 to 60 ^oC. Bacterial spores born on Venus may have found an ecological niche there. Droplets of water vapor would condense around the spores carried upwards, where the spores could become active and reproduce. When the water droplets grow and become heavy, they would fall back towards the planet, evaporating. The **naked spores** would thus be lighter, and could remain suspended until the next "awakening". If Venusian spores existed, with this mechanism they could explain the observation of this molecule in the upper atmosphere.

A further hypothesis assumes that the microorganisms that produce phosphine today were born on Earth and were launched into space by the impact of a meteor capable of making them escape into space. Once outside, attracted by the Sun, they could have spread into the Venusian clouds, populating them in a process of **panspermia**, already proposed for the origin of life on Earth [13].

2.2.2 Mars

The planet Mars, despite being smaller (∼11% of the Earth's mass), from a geological point of view had an initial evolution similar to the Earth and Venus: formed by aggregation of planetesimals, large bombardment of rocky and cometary bodies, volcanism with emission of lava and gas. Witness its atmosphere, typically made up of carbon dioxide, which has a composition almost identical to that of Venus and that of the primordial Earth.

Evolution of Mars

The birth of the planet and the formation of the oldest terrains took place between 4.5 and 3.8 Gyr ago. This period may have been dominated by a still warm environment and is characterized by large impact craters. The atmosphere of Mars may have formed

in the middle or late Noachian, around 3.8 Ga, due to the effusive activity of large volcanoes. We know today that the Martian atmosphere must have been denser, as indicated by fewer small impact craters than expected on a planet without an atmosphere. The shortage of smaller craters is caused by two effects: the first is the **fusion** of smaller mass meteoroids with atmospheric gases and the second is posterior to the fall and is caused by **atmospheric erosion**, which destroys its traces, leveling and erasing the smaller impact craters first and, over time, also the larger ones. A denser atmosphere in Mars' past would imply a greater greenhouse effect and a temperature capable of keeping the surface **liquid water**. In Noachis Terra and in the oldest soils of the southern hemisphere of the planet, a network of valleys is observed, similar to those carved by our rivers. The fluid that produced these valleys must have been common in the Noachian era due to the large number of structures observed. From the surface morphology it is possible to deduce that in an older period Mars must have had not only a dense atmosphere, but also surface water in a liquid state and perhaps a real ocean.

The subsequent Esperian period (3.7 Gyr-500 Myr) should have been much **colder** than the Noachian. From the study of the soils it can be assumed that about 3.7 billion years ago the temperature of Mars must have decreased considerably. A probable cause of this fact was the progressive disappearance of the atmosphere with the consequent decrease in the greenhouse effect. Unlike the Earth and Venus, born with a similar atmosphere, Mars would have undergone a progressive drying up, with the disappearance of much of the water from the atmosphere. The deviation from the evolutionary path of the Earth would lie in its lower initial temperature, but above all in the shorter volcanic season. The greater distance from the Sun, about twice that of the Earth, contributes to making it $\sim$ 40 degrees colder. Therefore a terrestrial greenhouse effect would not have been enough to keep surface water in a liquid state. But even if there were enough greenhouse gases to warm it globally above 0^oC, such a small planet would not have enough **internal energy** to power its volcanoes for 4.5 billion years.

In any case, once the volcanoes of Mars have stopped supplying the atmosphere with large quantities of gas, it is reasonable to think that the greenhouse effect has started to diminish. This led to part of the water vapor being incorporated into the ground in the form of **ice** and allowed carbon dioxide to be absorbed by the soil, removing greenhouse gases from the atmosphere. At the poles, when the temperature of Mars dropped below approximately -78 ^oC with a pressure of less than 100 hPa, carbon dioxide began to form dry ice and disappeared from the atmosphere in greater quantities. Some molecules have been split by the **solar UV radiation** and the atoms that compose them have escaped into space.

There may have been another cause for the gas escape: from the study of the reflectivity properties of rocks it seems that in the late Noachian there was a period of disappearance of the **magnetic field**, which may have allowed the particles of the solar wind to reach deeper in the atmosphere, favoring its escape outwards. The overall result of the dissipation or absorption of atmospheric gases was a greenhouse effect of just 3 degrees, with the disappearance of surface conditions favorable to life. Such a tenuous atmosphere and the consequent lack of greenhouse effect produce temperatures that can reach 27 ^oC in the tropics, in the summer and a few hours after noon, to diminish at the

poles reaching $-130\ ^oC$ overnight. Low atmospheric pressure prevents heat distribution and the vertical thermal gradient reaches 10 degrees between the ground and 1 meter high. On the ground the temperature it is higher when the sun heats the rocks and lower at night [13].

Possible life forms

In 1976, two space probes called Viking 1 and 2 landed in two flat areas of the northern hemisphere, in regions perhaps covered by the ancient Martian ocean. If Martian microorganisms exist and are similar to terrestrial ones, they can feed on organic substances present in the soil and produce carbon dioxide as in respiration or methane as for methanogenic bacteria. They can also absorb carbon dioxide from the atmosphere and transform it under the action of light to produce organic substances, as in photosynthesis. They can assimilate substances producing different types of gas with metabolic processes.

The three tools have been built on these three processes; the labeled gas release (LR), the pyrolytic release (PR) and the gas exchange (GEX). The results of the experiments show that possible microscopic life forms have probably been erased from the surface due to the changed environmental conditions, but could still exist where the conditions of chemical sterilization or solar radiation are absent: for example, they could live **underground**, where the internal heat can store water in the liquid state or under the ice caps [13].

Martian meteorites

Some terrestrial meteorites possess characteristics that indicate their origin from the planet Mars. They would have been generated by impacts of large objects that have launched fragments of rocks into space, where they are attracted to the Sun but ended up colliding with the Earth. The minerals within them are chemically modified, like the terrestrial rocks that arise from sedimentation or metamorphosis processes. These meteorites show traces of the processes undergone by wandering in space for thousands or millions of years.

A Martian meteorite, ALH 84001, collected in the Antarctic area of Alan Hills, shows an age of crystallization $\sim$ 4.5 Gyr, close to the birth phase of the planet. Originally formed from high temperature lavas, between 4.0 and 3.6 Gyr, was heated and deformed by strong pressure, probably due to the impact of a large meteorite or asteroid at the time of the Heavy Bombardment. After this shock, the material of ALH 84001 was covered with a fluid, presumably **water**, capable of generating mineral carbonate nodules.

This event could also be a consequence of the impact. Indeed, the formation of craters more than 65 km in diameter could dissolve enough water from the subsoil to create **temporary lakes** within the craters. Based on the existing environmental conditions, this water could freeze completely or evaporate after thousands of years, leaving mineral deposits in both cases. After this period, cracks are found in the crystals that would indicate a second shock with an age of $\sim$ 16 Myr and which could correspond to the impact that launched the rock into space. The journey between Mars and Earth ended $\sim$ 13 kyr ago, when ALH 84001 fell in Antarctica to be recovered in 1984 by a scientific

expedition.

Inside ALH84001 there are **stratified carbonate globules**, whose origin on Earth may be due to the action of bacteria or the evaporation of salt lakes, such as the Dead Sea. Inside the cells, the net carbon analysis after laboratory treatment has a residue $\delta C^{13} = -15$ %, attributable to chondrites falling to the ground or to biological activity. Associated with carbonates are polycyclic aromatic hydrocarbons (PAHs), substances also found in interstellar dust and which can result from the decomposition of living organisms. On Earth, they are abundant in sedimentary rocks, coal and oil deposits and result from the degradation of primitive plants and plankton. When the sediments in which the microorganisms are immersed transform into rock (**diagenesis**), thousands of types of PAH are produced, with different molecular weights. Various aspects of their distribution in the globules and in atomic weight would indicate their Martian origin.

However, it is possible to obtain PAH without biological activity, through reactions similar to an industrial process, called the **Fischer-Tropsch reaction**, which is catalyzed by magnetite (Fe_3O_4), an iron oxide found in the meteorite. When carbonate globules were observed under a scanning electron microscope, elongated ovoids ranging in size from 20 to 100 nm were observed, similar to fossil residues of nanobacteria found on Earth in travertine and limestone in general. These rocks are generated by evaporation of river water: as it evaporates, the calcium carbonate is deposited on the surface of plants and living materials. When the organisms disappear by putrefaction, they leave behind a porous rock.

However, these elongated structures have not been found in the other Martian meteorites, while they are present in the **Tatahouine meteorite**, which fell in the Sahara desert and collected in 1931, immersed or deposited on the calcite or silicates that compose it. These structures are ~ 3 times longer than those of ALH 84001, but are similar to those found in the soil of the Sahara near the collection area of the meteorite, residues generated by terrestrial bacteria, and not fossils. Also in this case it is difficult to distinguish between the hypothesis of biological and non-biological Martian activity [13].

2.3 Life on other planetary systems

In the first twenty years of the 21st century, thousands of planets were discovered. Planetary systems can present from two to seven planets and this phenomenon is quite common.

Some planets have even been found in the star system α Centauri, the closest to us (at just 1.3 pc from the Sun) and made up of three stars. Two are closest to each other, α Cen A, similar to the Sun (Type G), and α Cen B, orange (Type F). To them is added α Cen C, called Proxima Centauri, a red dwarf (Type M) that moves in an orbit 400 times larger. Proxima Cen has two planets: one similar to the Earth, in terms of radius, mass and a surface temperature that allows the existence of **liquid water** on the surface, and the other a super-earth of 7 $M_\odot$.

In the list of discovered planets, the **Jovians** and **Neptunians** are the most frequent, accounting for about 80%, with **earths** and **super-earths** in second place with less than 20%. Smaller planets exhibit negligible percentages. More than 70% of the planets are located at a distance of less than 0.4 AU from the star, which is equal to the one between

the Sun and Mercury. This proximity of the discovered planets is a bias due to the methods used, which measure the perturbation of the motion of the star by the planet: it is stronger the nearer and more massive the planet is.

However, this fact in the past years has led to questioning the **origin of planetary systems**, including the Solar System, in which the formation of planets was believed to take place on site, with the rocky planets close to the star being born from warmer material and without the gas, which had fled to the outer regions. Finding gaseous planets like Jupiter at such short distances from their stars, made researchers question about two fundamental topics:

- the resistance of the enormous layers of gases, that form their atmospheres, to the strong heat for the billions of years.
- the peculiarity of our planetary system, since all the others present different characteristics.

It was then understood how the planets, born in the protoplanetary disk, undergo the dynamic interaction of the surrounding material by dynamic friction, which causes them to lose energy, leading them in a spiral motion towards the star. Planets such as Jupiter would migrate inward passing on increasingly narrow orbits (**migration theory** or jumping jupiters). In the protoplanetary disk, however, there is a central area in which the high temperature of the star evaporates all the material, leaving a region free from dust and planetesimals. For a star like the Sun, this central "hole" of the protoplanetary disk is located within the orbit of Mercury. Once you get to that distance, the dynamic friction ceases and the planet remains in a more stable orbit. This would explain the accumulation of giant planets in regions too hot for their atmospheres.

Being very close to the star, a large part of the planets discovered are probably in **1:1 resonance**, always pointing the same hemisphere to the star. There is no sunrise or sunset on them and their Sun always remains fixed in the sky. Near the equator it is always summer, while at the poles it is perennial winter. On the dark side, the night is eternal. This orbital condition limits the variability of light and temperature of the planetary environment and can **affect the forms of life present**.

In addition, many known planetary systems revolve around **M-type red dwarf stars**. These stars, having less than 0.5 $M_{\odot}$, more easily reveal the presence of small planets. The planets of the M dwarfs are often terrestrial and sometimes numerous, as for example in the case of TRAPPIST1, with 7 planets of radius and mass similar to Earth. Some of them are in resonance with each other, like the great satellites of Jupiter.

Also stuck in a 1:1 resonance is the planet **WASP-67b**, which revolves at 9/100 of the distance of Mercury around a star hotter than the Sun (type F). The face facing the star reaches 2000 ^oC while the opposite face is at 1000 ^oC. The temperature is so high that the molecules are dissociated and the illuminated face is clear of clouds, while on the edge of the planet during the eclipse of the star the presence of gaseous iron was detected, which condenses into clouds and falls like a rain of iron, melted to the ground. This planet presents unfavourable condition for terrestrial forms of life.

Among the cases of discovered exoplanets, there is a particular one, the planet **S Orionis 70**, that belongs to the young cluster of stars σ-Orionis, which does not seem

to be linked to any single star. It is a hot object at 700 ^{o} C similar to a brown dwarf, with a methane atmosphere and a mass of $\sim 3\ M_J$. It may have been ejected from an unstable star system [13].

2.3.1 The habitable zone

In order to understand what kind of life can evolve in other planetary systems, it is possible to analyze the region around each star where a planet's surface temperature and preassure are similar to Earth's. This region, called the **habitable zone**, is made to correspond, in current research on exoplanets, to a strip of space in which water can exist in a liquid state on the surface of a planet. At pressures similar to the terrestrial one this occurs between 0 and 100 ^{o}C or 273 and 373 K, while at lower pressures this interval is progressively reduced. In this context, liquid water takes on the main role for the existence of living forms. In the Solar System this zone begins at 0.95 AU, just outside the orbit of Venus, and ends at 1.15 AU, just before that of Mars. The habitable zone naturally depends on the **energy emitted by the star**, its **radius** and the **greenhouse effect** generated by the planet's atmosphere and so on. All these parameters change over time, for instance:

- the brightness of a star can increase by 50% during its life;
- the stellar radius can extend during the red giant phase;
- the greenhouse effect vary with volcanic activity.

The discovered planets orbiting in the habitable zone of the nearest stars are the ideal place to look for life forms. **Terrestrial planets** or **rocky moons** around Jupiter planets could host terrestrial life forms.

Out of more than 4000 exoplanets, only 14% have a measure or estimate of the ground temperature, and only 2% of the total, about a hundred, have values that allow us to establish if they orbit in the habitable zone. If we narrow the selection to those with masses or dimensions similar to the Earth, they are just over a **dozen**. In some cases, the mass values are not known, so we assume similar properties to our planets: if the planet has the size of the Earth, will have a similar density, while the gaseous planets are much more extensive.

Of course, celestial bodies outside the habitable zone but with high **internal energy** or **underground oceans** are also possible candidates, even if it is very difficult to discover traces of life on their surface. For instance, the satellites Io, Europa and Ganymede derive much of their thermal energy from the tidal interaction with Jupiter and with the other satellites. In the subsoil of cold planets with an ocean and an internal energy source, there may be environments suitable for hosting life forms that do not need light.

Taking into account that terrestrial life forms show a wide spectrum of adaptation to the **most extreme environmental conditions**, it cannot be excluded a priori that a form of life, similar to ours, cannot exist in places that would be excluded from research using the habitable zone as a selection criterion [13].

The habitable planets

About twenty planets have been found in the habitable zone, presenting the favourable temperature and liquid water. If the gases incorporated in the rocks during the formation of the planet are able to create a volcanic atmosphere, then we would have all the ingredients for the birth of life. Having planets similar to the Earth is an excellent point of arrival of the path we have made, from the birth of the chemical elements to the molecules, up to the planets following in detail what has been the evolution of the Earth and Mars and of terrestrial life forms. However, it is not enough.

It is necessary to analyze the atmospheric gases present on an exoplanet by observing which spectral lines or bands appear or disappear in its orbit. In the microwave range, where stars like the Sun are less bright, it is possible to study the molecules present in the atmosphere through radio telescopes. We are therefore theoretically able to know not only how big, dense and hot the planet is, but also what its atmosphere is made of. In our Solar System, the spectrum of Neptune or Jupiter shows ammonia and methane, that of Mars and Venus carbon dioxide, but the spectrum of the Earth has unique characteristics: there are traces of water vapor, molecular oxygen and ozone.

Traces of water suggesting rain have been observed, for example, on planet **K2-18b**, a super-earth orbiting a red dwarf.

The presence of bacteria and plants that use photosynthesis leaves a very evident trace in the absorption and reflection of sunlight. **Chlorophyll** creates a marked absorption in the infrared near 800 nm, which is called "red edge". In images taken with filters with very small wavelength bands, it can be seen that from 700 to 800 nm there is an absorption jump. Observations so far have revealed the presence of many molecules:

- in the planets around the hottest stars there are traces of atomic carbon, iron and other metals;
- in those with stars similar to the Sun, traces of water, sodium, potassium and oxygen;
- in those of the red dwarfs methane, carbon monoxide and water appear.

The presence of chlorophyll or ozone has not yet been observed. If it happened, this would be a great leap forward for Astrobiology. However, we can develop theories on what the life forms of these planets could be, based on what we know about the evolution and development of terrestrial life [13].

The effect of gravity

Some of the planets discovered are hastily referred to as "a second Earth". But similar dimensions and radii are not enough, because the largest terrestrial organisms are sensitive to the **acceleration of gravity**. A small variation in size or density is enough to completely change the planetary environment with respect to our planet. For a small sample of terrestrial planets, the value of the gravity that varies from 86% to 160%. If we consider a person of 70 kg on Earth, on the surface of the most massive planet, **TOI 700d**, this person would weigh 112 kg, and it would be difficult and tiring for him to

even walk. On this planet, in addition to bacteria and other microscopic animals, there may only be crawling, skeletal, or very massive animals that can withstand that force of gravity. There would be no tall trees and probably no birds or flying insects. Consequently, as flowers are pollinated by insects on Earth, it is possible to think that there are no flowers on TOI 700d, no palm trees either orchids. Perhaps only the seas would give respite to the great weight, with greater hydro-static thrust.

At the other extreme, on a planet with a lower density than Earth such as **TRAPPIST 1f**, the same 70 kg human would weigh 43 kg. We know from experiments at the International Space Station that lower gravity causes damage to the skeletal system, heart and muscles. Living in lower gravity will make tall beings grow, but for us earthlings it would be harmful. Tall plants and animals could develop, and insects and birds, but very different from ours.

Only on planets such as Proxima Cen b, Teegarden b and c, TRAPPIST 1g and TOI700b and c does the force of gravity ensure an environment that is physically similar to ours. However, these are not ideal planets for terrestrial life, because their stars, **red dwarfs**, are much smaller and colder than the Sun. Water will be liquid only on the surface of the planets closest to the star, where the heat is maximum. However, in this condition, most of the planets present 1:1 planet-star resonance or various resonances between planets. This would imply that half of the planet presents hot temperatures and the other half frozen environment. The bright disk of the star may appear in the sky 3 to 5 times larger than the Sun. But on the planets just mentioned as most similar to Earth so far known it will be dominated by a **red light** that spreads over everything, without sunrise or sunset, a cool or cold air, anoxic atmosphere, with dangerous flashes of energy from the sky [13].

Chapter 3

Lithopaspermia

We mentioned that the Earth was initially too hot and the volcanic water completely sterile to release molecules as complex as nucleic acids or amino acids in the oceans of the Archean. Thus it becomes necessary to postulate help from space to form the necessary molecules, perhaps in the form of small comets or cosmic dust. Therefore, the Earth would not be the generator of life, but only its **cradle**, in which already elaborated substances have found the favorable conditions to assemble: a stable temperature, water in a liquid state and a continuous supply of energy, sufficient to stimulate chemical reactions but not so powerful as to destroy the substances involved. In that case, amino acids, nucleic acids and lipids would all be available simultaneously, without the need to expect that one of them was the precursor of the others [13].

Thus we can say that the **panspermia** theory is based on the idea that life and water derived from the external and cold part of the Solar System, as asteroids, comets and dust, and were deposited on a barren Earth after its cooling. In particular, we want to study the **lithopanspermia**, thus the possibility of interplanetary transport of microorganism via asteroids (Fig. 3.1). It involves three basic teps [16]:

- the **escape process**, that implies that the biological material is removed from the surface of an habitable planet and survives after being lifted to higher altitudes by impact ejection;

- **interim state in space**, so the survival of the biological material over time scales comparable with interplanetary or interstellar passage;

- the **entry process**, in which the biological material is deposited on the surface on another habitable planet without being destroyed.

All three main topics of lithopanspermia are now accessible to experimental testing in ground simulation facilities as well as in exposure experiments in space.

The possibility of meteorite-mediated interplanetary transport of life was already theorized in the 1870s by von Helmholtz and Thomson (Lord Kelvin), who supported the panspermia in which fragments of extraterrestrial rocks transporting microbes as **blind passengers** within their cracks, may carry life from one planet to the other. However,

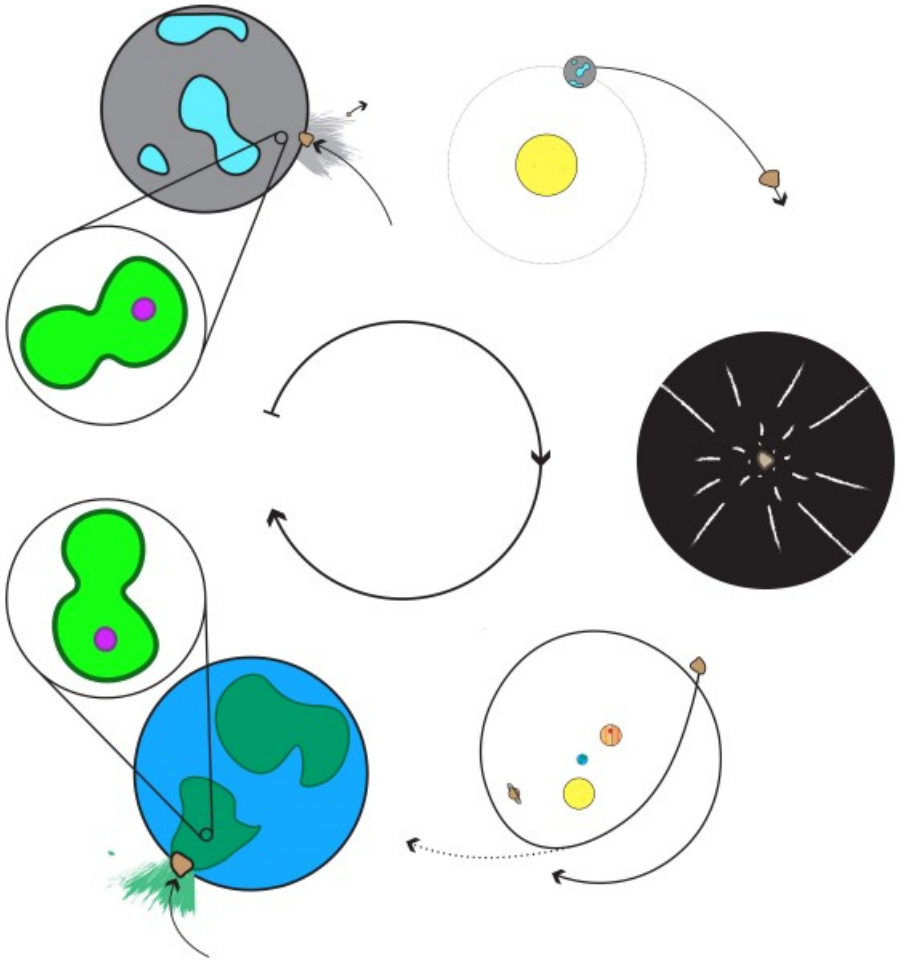

Figure 3.1: Schematic diagram representing the processes at the base of a successful transfer of life from one planetary system to another (proceeding clockwise from the upper left to the lower left). First of all, life must arise on a habitable planet. Rocks that contain living biological material must then be removed and then ejected from the planetary surface. Then it is expelled from the planetary system. After traveling through interstellar space, the asteroid must be captured by another planetary system and collide with the surface of a potentially habitable planet. Finally, the biological cargo must thrive in its new environment. [5]

during their lifetime, no mechanism was known to accelerate rocks to escape velocities in order to leave their planet of origin; as a result Kelvin's idea was discarded [13].

After the discovery in 1983 that a certain group of meteorites, the so-called *SNC*

meteorites, has originated from Mars, evidence was provided that rocks can naturally be **transferred between terrestrial planets** in conditions that could maintain trapped viable life systems, and as a consequence, Kelvin's idea, now called Lithopanspermia, has been revisited [16].

We know that substances similar to those necessary for life are present in the interstellar clouds from which stars and planets are formed. Therefore nothing prevents us from thinking that they existed in the **colder areas** of the protoplanetary disk of the Solar system. Confirmation of this presence comes from the discovery of amino acids, nitrogenous bases and in general of substances similar to biological ones within carbonaceous chondrites. As in the case of ocean water, some or all of the prebiotic substances could have arrived on an Earth, that has been sterilized by the heat of the impacts, only after its cooling, transported by asteroids.

3.0.1 Previous studies on lithopanspermia

It has been argued that the probabilities that a microbiological cargo can be transferred between solar systems is very low due to the long distance, huge amount of time and low interstellar density (Melosh 2003 [21]). The results of his numerical simulation indicate that among all the meteorites ejected from terrestrial planets, only about one-third escape from the solar system due to the gravitational perturbation of giant planets as Jupiter and Saturn. Even if we consider the Heavy Bombardment phase, the asteroids ejected from terrestrial planets would have 10^{-4} probability to land in an host planetary system. Therefore, Melosh concluded that the lithopanspermia between solar systems is 'overwhelmingly unlikely', while the origin of life on earth must be sought within the solar system boundaries.

The transfer of material ejected from terrestrial planets has been accurately analyzed by Worth et al. [37], who discovered that the launched material frequently collides with other terrestrial planets, and with the moons of Jupiter and Saturn but with a lower rate. Such transfer is more likely during the Late Heavy Bombardment, when the icy moons were warm enough and presented a small layer of ice to prevent the asteroids from reaching the internal liquid shell.

For the interstellar transfer of life, other researchers investigated the likelihood of this mechanism and came to the conclusion that is is hugely enhances while dealing with more **crowded stellar environments**, as suggested by Adams and Spergel [4]. In particular, they analyzed the lithopanspermia hypothesis in star-forming star clusters , where the close proximity of the planetary systems and the relatively low velocities between them highly enhances the probability of transfer of life via asteroids. Moreover, their model presents the cluster lives for only 10-100 Myr, so the timescales for the transfer are shorter and the presence of binaries increases the cross section for the capture of the planets.

Another supporter of the interstellar panspermia is the scientist W. M. Napier [25], who simulated meter-size boulders that have been launched from an Earth-like planet by large impacts, destroyed by collisions and eroded by impacting zodiacal cloud dust particles. Once their dimension is reduced to a critical value (of the order of one micron), the particles are rapidly ejected from the solar system due to radiation pressure. The critical size is large enough to protect the microorganisms from the UV radiation. During their

travel in the interstellar regions, the particles may be incorporated into **protoplanetary systems**, shielded by cosmic rays inside the growing planetasimals: the microorganisms are deposited in small but dense molecular clouds. This phenomenon can be the leading step in a chain reaction, favouring the seeding of the disk of the Galaxy within few billion years.

3.0.2 Physical properties of the carrier

The chemical composition

Minerals from micrometeorites can incorporate organic material, and even if they degrade while falling to the ground, they are still able to **protect** it. Of course it also depends on the speed of falling to the ground, tens of km/s, and on the composition and density of the atmosphere that can burn the dust by friction.

The primordial atmosphere of the Earth had to be volcanic, with abundant water vapor and carbon dioxide, very different from the primordial atmosphere of ammonia and methane predicted in Miller's experiment. However, it is likely that a remnant of the primordial atmosphere may have initially stayed at high altitudes. An atmosphere of this type, with lighter molecules, can **favor the passage of micrometeorites**, braking them without excessive heating and consequent destruction of the substances they carry. Among the candidate materials to be the vehicle of prebiotic substances there are:

- **carbonate granules**, as magnesite, calcite and siderite;
- **silicates**, as forsterite and fayalite;
- **sulphates**, as anhydrite.

The latter minerals, capable of incorporating water and organic molecules, according to recent studies can resist the entry into the atmosphere while remaining **partially unaltered** and allowing the organic material to accumulate on the ground [13].

The total mass of the ejected rocks

According to previous simulations of the late stages of planet formation and analysis of the disk substructures, the total amount of mass that can be launched by a star/disk system M_R is $\sim$ 1-10 $M_\oplus$ and can be represented by the equation:

$$M_R = f_R \, M_\oplus, \tag{3.1}$$

where f_R is a factor of the order of unity [5].

Every planet will eject only a fraction of the total amount of launched mass M_R, and only a fraction of this quantity will be biologically active. Our purpose is to analyze the evolution of the life-bearing asteroids, that may contain substances as spores, seeds, DNA, algae, fungi, lichens and so on. The ejected mass of the biological cargo can be expressed by the formula:

$$M_B = f_B \, M_R = f_B \, f_R \, M_\oplus \tag{3.2}$$

where the exact value of the quantity f_B is uncertain, but we are interested in the order of magnitude, that is usually $\ll 1$. If we assume that the habitable planet shares similar properties to the Earth, the total mass of the biosphere is around $10^{-10}\ M_\oplus$ [1]. However, only a fraction of the biosphere mass is ejected, and only a small component of the mass in the asteroids has biological microorganisms. Therefore, it has been estimated an upper limit for f_B given by $f_B < 10^{-10}$.

To infer the lower limit, it is necessary to compute the mass loss rate of an Earth-like planet for the entire age of the solar system. According to previous studies, around 15 biologically active rocks, with masses $\sim 10^4$g, are ejected from the planet every year. If we integrate this amount for the age of the solar system, the total ejected mass will be of the order of $10^{-13} M_\oplus$. This means that f_B will range between the values:

$$10^{-13} < f_B < 10^{-10} \tag{3.3}$$

This range is conservative and subjected to the peculiarity of the evolution of every single planed. For instance, if the planet becomes habitable in the early stages of its life and undergoes frequent impacts, then the ejected biological cargo can be a larger fraction of the mentioned quantities. In some extreme cases, the integrated biological mass over time can exceed the instantaneous mass of the biosphere of the Earth. As an alternative, the biosphere on the Earth can be deeper or more extended, enhancing the lithopanspermia [5].

Distribution of rock sizes and masses

Before we estimated the total mass of ejected material from an Earth-like planet. Now we want to evaluate the probability of biological transfer, so it is necessary to specify the number of rocky bodies that could in principle be the transporter of the biological cargo.

The size distribution of the asteroids is a steep decreasing function of the radius (and therefore of the mass). The **lower mass limit** necessary to safely transport microorganisms highly influences the overall number of rocky bodies for a given total mass.

According to previous studies, the minimum rock mass has been estimated to be $m_{min} = 10^4$g, (e.g. Horneck 1993 [15], Nicholson et al. 2020 [26]). This lower limit provides a measure of the mass of the rock that enables the microorganisms inside it to survive, guaranteeing [5]:

- a **shield** of the biological cargo from the interstellar cosmic background;
- the **survival to impact events** that consists in the collision and in the subsequent ejection from the Earth-like planet;
- after being captured by another planetary system, the asteroid must survive to the **re-entry process** onto the surface of the receiving planet.

[1] This biomass is mostly characterized by land plants. Theoretically, the seeds can be enclosed within rocks and travel in the space, but we do not have enough experimental data. Moreover, it is important to underline that the land plants have lived on the Earth for 10% of the planet's existence [5]

The mass distribution of the asteroids can be approximated to a power-law, described by the equation [5]:

$$\frac{dN}{dm} = Am^{-p} \tag{3.4}$$

where the power-law index p ranges between 1 and 2 and A is a normalization factor. In particular, in the case of collisional processes, the estimate of the power-law index is $p \approx 1.8$. If we observe the distribution of objects colliding with the upper layer of the atmosphere, the power-law presents an index of $p \approx 1.7$.

The mass distribution in Eq. 3.4 reveals that most of the mass is contained in the rare largest objects, while the smaller ones are more frequent. We can define the upper mass cutoff m_2 and a lower mass cutoff m_1, and we can express the normalization factor as function of them, according to the approximated equation [5]:

$$A = \frac{(2-p)M_R}{m_2^{(2-p)}} \tag{3.5}$$

and the overall number of asteroids per star is expressed by:

$$N_{R\star} = \frac{(2-p)}{(p-1)}\left(\frac{m_2}{m_1}\right)^{p-1}\frac{M_R}{m_2}. \tag{3.6}$$

If we assume that M_R is the total mass of the rocks ejected from a given system, then $M_R \sim M_\oplus$, as mentioned before. Substituting the value of M_R, m_1 and m_2 (that in general goes around 0.1 $M_\oplus$), we obtain a value of $N_{R\star} \sim 10^{16}$ [5].

3.0.3 Distribution of the ejection speed

We can model the general form of the distribution of ejection speeds with the following heuristic argument, based on the idea that the ejections occur through close encounters between the planets. We can define b as the impact parameter of these interactions, so that the ejection speed can be written in the form [24]:

$$\frac{1}{2}v_{ej}^2 = \frac{\alpha G\langle m\rangle}{b} - \frac{G\,M_\star}{2a}, \tag{3.7}$$

where a is the semi-major axis of the ejected planet before the interaction, $\langle m\rangle$ is an average mass of the remaining planet, and α is a dimensionless factor of order unity, that depends on the geometry of the interaction.

We can then define the velocity scale v_P^2 and a length scale r_0 respectively [24]:

$$v_P^2 \equiv \frac{G\,M_\star}{a} \tag{3.8}$$

$$r_0 \equiv 2\alpha\left(\frac{\langle m\rangle}{M_\star}\right)a \tag{3.9}$$

Therefore, the ejection speed can be described by the equation [24]:

$$u = \left[\frac{1}{\xi} - 1\right]^{\frac{1}{2}} \tag{3.10}$$

where $u \equiv v_{ej}/v_p$and $\xi \equiv b/r_0$.
Assuming that the target is circular, the probability for the ejection [24]:

$$F(u) = \frac{4\,u}{(1+u^2)^3} \tag{3.11}$$

This probability distribution is normalized to unity over the full range of dimensionless ejection speeds $0 < u < \infty$. In practice, the minimum value of the impact parameter is given by the radius of the ejector planet, $b_{min} = r_P$, with the corresponding cutoff in the ejection speed $v_{max} \approx v_P\,(r_0/r_P)^{\frac{1}{2}}$. However, the distribution of the ejection speed falls rapidly at high values so that the estimate of this cutoff is relatively unimportant [24].

Chapter 4

Dynamical evolution of the cluster

Star clusters are the birth place of stars, collecting from hundreds to millions of stars and they affect the evolution of the asteroids in our simulation.

The dynamical evolution of star clusters has a key role in our study for several aspects (Adams and Spergel, 2005 [4]):

- The **density** of solar systems is much greater than in the Galactic field, and the **relative velocities** are lower, thus enhancing the transfer of any asteroid
- most stars reside in **binaries**: they increase the cross sections for the capture of passing asteroids
- the **background UV radiation fields** are stronger in regions of clustered star formation, hence the biological cargo is in greater danger

Clusters form from a gravitationally bound cloud that fragments into stars in a few **crossing times**, that are a measure of how the system reacts to global changes in its potential.

The cluster can be described by the following parameters [35]:

- the **virial radius**, that is a measure of the cluster scale:

$$r_{vir} = \frac{GM^2}{2|U|} \tag{4.1}$$

  where G is the gravitational constant, M the mass of the cluster and U the total potential energy;

- the **core radius**, that represents the distance from the center at which the surface brightness [1] reduces by half of the central value

$$r_{core} = \sqrt{\frac{3\langle v^2 \rangle_o}{4\pi G \rho_0}} \tag{4.2}$$

[1] The surface brightness is defined as the total stellar luminosity emitted per unit area of the disk (Binney and Tremaine, 2008 [7]

- **Lagrangian radii**, that are an indicator of the percentage of the total cluster mass enclosed inside a given radius: the 25th Lagrangian radius encloses the 25% of the total mass, the 50th one contains the 50% of the cluster mass and so on.
- **tidal radius**, that defines the outer limit beyond which the stellar density drops to zero;
- **truncation radius**, the limit beyond which stars are stripped from the cluster due to the Galactic tidal field.

The evolution of stellar clusters is driven by two fundamental time scales: the crossing time and the **two-body relaxation time**, that indicates a temporal scale in which the overall two-body encounters significantly modify the individual stellar orbits [12].

4.1 Two body relaxation

We analyze the evolution of a collisional system, where the stars can experience **encounters**, that are gravitational perturbations of their orbit due to a close fly-by of another star, and **collisions**, that are actual physical mergers between stars.

Individual stellar encounters are therefore responsible for a gradual deviation from the trajectories that the stars would have taken if the gravitational field were perfectly smooth. For this reason the stars diffuse in phase space away from their original orbits (Binney and Tremaine [7]). If we integrate this effect for million years, after many such encounters every star eventually loses its memory of the original orbit and ends up describing a trajectory totally unrelated to the original one. The characteristic time over which this loss of memory occurs is called **two-body relaxation time** t_{relax}, that is defined by the formula:

$$r_{relax} = n_{cross}\, t_{cross}, \tag{4.3}$$

where n_{cross} is the number of crossings that is required to have a velocity variation of the order of the initial velocity of each star (i.e., $\delta v \sim v_0$) and t_{cross} is **crossing time**, the time needed for a star to cross the galaxy once, described by respectively:

$$n_{cross} = \frac{N}{8 \log N} \tag{4.4}$$

$$t_{cross} = \frac{R}{v} \tag{4.5}$$

where N is the total number of stars in the cluster, R the galactic radius and v the typical velocity of the stars. This model is valid under the assumptions of spherical symmetry, not rotating system and composed by identical stars (Binney and Tremaine [7]).

In case of measuring the relaxation time for a population of **identical stars of mass** $m_\star$ and with a Maxwellian velocity dispersion σ, we use the formula in Eq. 4.6, where σ^2

is the mean-square velocity in any one direction, G the gravitational constant and ρ the stellar density.

$$t_{relax} = 0.34 \frac{\sigma^3}{G^2 \rho \, m \ln \lambda} \tag{4.6}$$

For timescales higher than t_{relax} the gravitational potential cannot be approximated as smooth.

4.2 Dynamical friction

In addition to the two-body relaxation, if the stars present a certain distribution in mass, there is another effect that drives the evolution of the cluster: **dynamical friction**. Dynamical friction is a drag force that reduces the velocity of massive stars in stellar clusters (Binney and Tremaine, 2008 [7]).

When a particle with **mass M** travels within an infinite and homogeneous grid of **lighter bodies of mass m**, it attracts the lighter particles, leaving a local over-density behind it. The massive particle is subject to a force parallel and opposite to the initial velocity v_0 from the over-density and slows down. This phenomenon is responsible for the deceleration of the most massive stars, that sink to the center of the star cluster, and the acceleration of the lighter ones, that expand outward (the so-called '**evaporation**') [20].

The typical timescale of the dynamical friction is expressed in Eq.4.7 (Chandrasekhar, S. 1943 [8]):

$$t_{df} = \frac{3}{4(2\pi)^{\frac{1}{2}} G^2 \ln \lambda} \frac{\sigma^3(r)}{M \rho(r)} \tag{4.7}$$

The dynamical friction and the two-body relaxation are correlated: if we compare Eqs. 4.7 and 4.6, we can introduce a formula that expresses the link between the two phenomena:

$$t_{df} = \frac{m_\star}{M} t_{relax} \tag{4.8}$$

where $m_\star$ is the average mass of the stars in the cluster, while M is the one relative to the massive stars in the dynamical friction explanation. It means that relaxation is a similar phenomenon to dynamical friction: the first one deals with the overall and average interactions between stars, while the second studies the relation between a massive star M and the other lighter stars.

4.3 Mass segregation

As a consequence of dynamical friction, we have the so called **mass segregation**, that refers to the mass distribution of the stars in the cluster (Portegies Zwart et al. 2010 [31]): massive stars concentrated in the center, low mass stars in the outer parts.

Within this framework, as consequence of the increase of the density of massive stars close to the center of the cluster, the instability of the system increases and the core collapse is enhanced: the inner part of the cluster presents a higher collision rate, an

increase of mass loss and more interactions between the stars, leading to binary formation [2] [20].

On larger scales, the dynamical friction could cause the sinking of star clusters to the center of the host galaxy. As a result, the nuclear star clusters (typical masses $\sim 10^4 - 10^8$ and few Gyr old), that are generally located at the center of galaxies like the Milky Way, might be the result of the assembly of smaller star clusters.

It is known that a cluster can also present a **primordial mass segregation**. This means that there is a higher concentration of massive stars in the center of the cluster since the beginning, and this can be verified by comparing the dynamical friction time scale for stars of a certain mass limit m with the cluster age: if the time scale is higher, the mass segregation is primordial (Portegies Zwart, McMillan and Gieles 2010 [34]).

4.4 Stellar evolution

One of the reasons behind the decrease of the clusters radius over time is **stellar evolution**: the stars, during the stages of their life, loose large fraction of their mass by stellar winds or supernovae explosions. This mass is expelled from the cluster, that implies the decrease of the truncation radius [12].

[2] The two-body relaxation is responsible for a velocity distribution of the stars close to a Maxwellian one. The stars in the high velocity tail are continuously ejected by the galactic tidal field, causing the decrease in the radius of the cluster and an increase of the concentration of the stars [12].

Chapter 5

The AMUSE environment

The Astrophysical Multi-purpose Software Environment (AMUSE) is an open-source component library and community effort with the aim of performing high quality simulations in astrophysics [35].

Many areas of computational astrophysics require simultaneous solution of systems of equations covering multiple physical domains, that may span broad ranges in length and time scales. Moreover, the separate domains may be tightly coupled on the scales of interest and the combination of many competing physical processes and large dynamic range, together with the sheer size of the computation, represent a major theoretical **challenge** for computational astrophysics. As simulations and data analysis become progressively complex, computational scientists face an increasing need for flexible frameworks capable of integrating new and existing scientific codes, together with allowing scientists to easily build their simulation workflow [33].

The targets of interest can be dense stellar environments in which gravitational dynamics, radiative processes, stellar physics, and gas dynamics all play important roles. Spatial and temporal scales range from 10^3 m and 10^{-3} s on the small end to 10^{20} m and 10^{17} s at the other extreme. Close encounters and physical collisions among stars and binaries are recurrent, and large and small scales are intimately coupled by stellar mass loss, binary heating, stellar collisions, dynamical mass segregation, and core collapse. The number of stars can exceed 10^6 in many cases [33].

It is possible to combine all these elements within a large-scale simulation of such a system, but it could pose significant software development problems. The present generation of cluster simulation packages (often called **kitchen-sink** codes) have been very successful in modeling the long-term dynamical evolution of star clusters, from a few Myr after formation to their eventual dissolution in the Gyr later, due to the galactic tidal field. These packages include both N-body and Monte Carlo codes, with sophisticated solutions for stellar dynamics and binary/multiple interactions, but these are generally coupled with much more approximate treatments of other physical aspects of the system. For instance, stellar evolution is typically evaluated as a look-up from precomputed results, while binary evolution consists in a set of rules of varying accuracy, implemented on top of the stellar evolution subsystem [33].

Other aspects of the simulation, such as stellar collisions, are developed more approximately: stars are modeled as spheres that merge when they collide, preserving virtually none of the underlying stellar physics.

An additional limitation of most kitchen-sink codes is that specific implementations of each physical process are hard-coded into the simulation, so adoption of a particular package implies a particular choice of dynamical integrator, stellar modeling, binary evolution, and so on.

The individual modules in AMUSE contain dedicated and efficient implementations of specific pieces of the calculation, and are linked by a high-level scripting language to guarantee flexibility and facilitate management. Modules can contain wrapped legacy code or new code developed specifically for the project, and all have a standard interface exposing only necessary functionality, allowing them to be easily mixed and replaced as needed [33].

The term 'community code' refers collectively to public domain codes encompassed by the AMUSE framework.

5.0.1 The AMUSE Software Framework

The global structure of the AMUSE environment is described in Fig. 5.1.

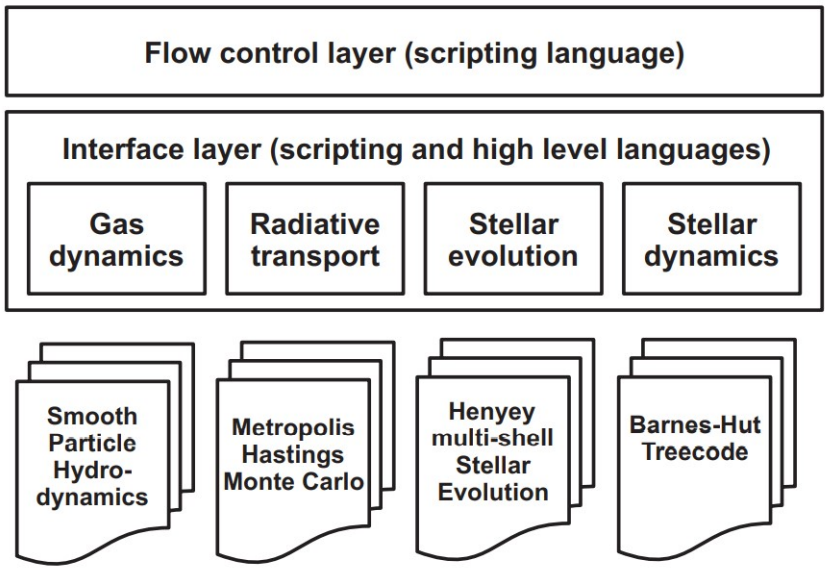

Figure 5.1: The AMUSE environment. The top-level flow control layer is a custom GUI or user-written Python script that specifies the structure of the program, replacing the top-level loop of a traditional program. Each of the four physics areas shown in the interface layer may be instantiated by one of several modules, allowing arbitrary combinations to be explored. [33]

In the AMUSE programming model, each physical process (advance the stellar or hydrodynamics to a specified time, evolve a star, collide two stars, etc.) is implemented

as a module with a standard interface onto the rest of the system, but the details are private to each module. For instance, all stellar modules include accessor functions that provide information on the mass and radius of a specified star, but the details of what a star is (an analytic formula, or a set of 1D or 2D arrays describing the run of density, temperature, composition, etc.) are internal to the module and are normally invisible to the user. Objects within each module are identified by a **global ID**, and it is the responsibility of the module implementation to provide the required accessor functions for a specified ID.

The AMUSE language is **Python**, ease of programming and rapid prototyping, large user base in the astronomical community, and extensive user-written software. The design of AMUSE applies no restrictions on the choice of language for any given module, except that it must support the parallel Message Passing Interface (MPI).

In a typical application, the top-level loop (**the flow control layer** in Figure 5.1) of a simulation is written entirely in Python, allowing monitoring, analysis, graphics and other Python tools to be implemented. The modular design and the use of private internal data highly reduces both the computational overhead of the Python code segments and data flow between modules. The relatively low speed of the language does not significantly impact the outcome, because all of the computational load is supported by the (high-performance) modules.

Most of the computational scientists are familiar with the concept of modular software frameworks for program integration, maybe less known is the use of MPI as the communication tool among modules. In the initial implementation of AMUSE, individual modules written in Fortran 77, Fortran 90, Fortran 95, C, and C++ were interfaced with Python using *f2py*[1] or *swig*[2]. This approach works well for simple demonstration programs, but it has a number of serious technical drawbacks when deployed in a parallel, high-performance environment [33]:

- imposes namespace restrictions that can lead to conflicts between independent modules;
- makes it impossible to instantiate multiple independent copies of a given module;
- rules out incorporation of parallel modules into the AMUSE framework.

All of these problems can be avoided by replacing the standard *swig/f2py* interface with an explicitly parallel structure in which **MPI** is used throughout the AMUSE system for communication between all modules (serial or parallel). One of the advantages of using MPI is its easily availability, accurate documentation and wide usage in the astronomical community.

As a result, AMUSE is characterized by serial and parallel modules are indistinguishable one another, as seen from the flow control level (Figure 5.1), making them easy to combine, largely transparently to the user.

[1] See http://www.mcs.anl.gov/mpi

[2] See http://www.scipy.org/F2Py and http://www.swig.org.

Currently, AMUSE contains at least two independent modules for each physical process, allowing **interchangeability** between implementations. This approach enables direct comparison and calibration of different implementations of the same physical processes, and facilitates experimentation in constructing new models.

In a star cluster simulation typically carried out by kitchen-sink codes, the python script acts as a scheduler for the stellar dynamical and stellar evolution modules and intervenes when unscheduled events, as collisions or supernovae, occur.

In most cases there is no need for communication between modules beyond the data transferred through the standard interface. However, in some circumstances it is needed additional information, as it could be required when the collision and stellar evolution modules may need to exchange detailed structural data before and after a physical stellar collision.

Chapter 6

Method

We perform a numerical simulation of a uniform sphere of asteroids in a dense stellar cluster that is dynamically influenced by the galactic tidal field.

6.1 N-body simulations

For N-body simulation we denote the numerical integration of the forces acting on N particles for a certain interval of time t. It can be applied to multiple fields, as astrophysics, fluid-dynamics, molecular dynamics and so on [20]. In particular, in astrophysics the force we consider is the gravitational one, that is a long-range force described by second order, non linear, singular ordinary differential equations, where the acceleration felt by each particle a_i is described in Eq.6.1,

$$a_i \equiv \ddot{r} = G \sum_{j \neq 1}^{N} m_j \frac{r_j - r_i}{|r_j - r_i|^3} \tag{6.1}$$

where G is the gravitational constant, r_i the position of particle i, r_j and m_j the position and mass of particle j respectively. The bodies can be stars, planets, gas, dark matter and so on. In the specific case of gas evolution, we would need to implement Euler equations too, but this study will not include gaseous bodies.

6.1.1 Approximations

Our simulation is based on the evolution of a stellar cluster that probably shares the same initial conditions as the one where the Sun was born. Since N-body integrations are extremely expensive when dealing with thousands of particles, we assume the following approximations (Portegies Zwart and McMillan, 2018 [35]):

- we consider that all the particles are point-mass objects and the center of mass is exactly their geometric center, neglecting their non-sphericity and spatial extension. In our study, the **point-mass approximation** does not lead to large errors.

- All the **relativistic corrections** implemented by Einstein to the Newtonian model are not taken into account: we ignore any relativistic effects and apply the pure Newtonian dynamical force described in Eq.6.1.
- the **speed of gravity**, that is the speed with which the gravity propagates, is infinite in the case of our N-body simulation, while in Einstein's general relativity it is equivalent to the speed of light [1].

6.2 Milky Way

The tidal field of the Milky Way is responsible for the dissolution of the star clusters.

The potential of the Milky Way can be described with a semi-analytic code based on the **composite bar** model, [32] that is the result of the superposition a bar and an axisymmetric component, that includes the bulge, disc and dark matter halo. The potential is based on the considerations by Allen and Santillan, 1991 [6] to fit the axisymmetric component of the Milky Way.

The **bulge** and the **disc** potential are described with the model provided by Miyamoto-Nagai 1975 [23]:

$$\Phi_{bl}(R,z) = \frac{-GM_b}{\sqrt{(R^2 + b_1^2 + z^2)}} \tag{6.2}$$

$$\Phi_d = \frac{-GM_d}{\sqrt{(R^2 + (a_2 + \sqrt{(z^2 + b_2^2)})^2)}} \tag{6.3}$$

where (R, z) are the cylindrical coordinates, M_b and ,M_d are the bulge and disc mass respectively, b_1 is the bulge scale length, a_2 and b_2 are the radial and vertical scale lengths, respectively.

The **dark matter halo** is developed with a spherical potential [32] (Eq.6.4):

$$\Phi_h = \frac{-G(\frac{M_h}{a_3})d_1^{1.02}}{(1 + d_1^{1.02})} - \frac{GM_h}{(1.02a3)}\left(- \frac{1.02}{c} + \log(c) + \frac{1.02}{(1 + d_1^{1.02})} - \log(1.0 + d_1^{1.02})\right) \tag{6.4}$$

where the halo radius is 100 kpc, M_h is the halo mass and a_3 is its scale length. The parameters are chosen so that the total mass of the axi-symmetric component is 9×10^{11} $M_\odot$ and the rotation curve flattens at approximately 200 km/ s, setting the Galactocentric distance to the Sun $R_0 = 8.5$ kpc and the circular velocity at the Sun's position to $v_0 = 220$/s.

All the quantitative values of previous parameters are listed in Tab. 6.1.

[1] The speed of gravity c_{gw} is the speed of the gravitational waves, and in the case of Lorentz-invariant solution it is equal to the speed of light. However, in our Universe, the Lorentz-invariance is broken and the speed of gravity depends on the medium through which the waves propagate. In particular, measuring the c_{gw} is a fundamental tool to estimate the composition of our Universe (Harry and Noller, 2022 [14])

Parameter name	Value	Unit
Halo cut-off	100	kpc
Scale length bulge b1	0.3873	kpc
Scale length disk a2	5.3178	kpc
Scale length disk b2	0.25	kpc
Scale length halo a3	12.0	kpc
Mass Bulge	1.40592 x 10^{10}	$M_\odot$
Mass Disk	8.5608 x 10^{10}	$M_\odot$
Mass Halo	1.07068 x 10^{11}	$M_\odot$

Table 6.1: Parameters for the Milky Way potential

6.3 N-body modelling of a star cluster

6.3.1 Initial conditions

Every cluster of stars forms from the collapse of a molecular cloud and after few dynamical times the system gets in virial equilibrium, in which any substructure related to the initial phase of the formation of the cluster is disrupted. After few million years from the birth, the stellar cluster presents a well defined structure, that can approximated to a spherically symmetric object. This is the reason why we decide to adopt a **Plummer sphere** [28] as initial condition for the density profile of our cluster, neglecting the initial phase of the interstellar cloud because too computationally expensive and not relevant for our purpose.

The cluster evolution starts with a total number of stars $N = 2500 \pm 300$ and a virial radius equal to $r_{vir} = 0.75 \pm 0.25pc$, since these are values that probably best represent the birth cluster of our solar system (Portegies Zwart 2019 [40]).

As initial mass function for the **mass distribution** of the stars, we adopt the model proposed by Kroupa 2001 [18], that can be described by the multiple-part power-law Initial Mass Function (IMF) in Eq.6.5:

$$\xi(m) = m^{-\alpha_i} \tag{6.5}$$

where $\xi(m)$ dm is the number of single stars in the mass interval m to m + dm and
$\alpha_0 = +0.3 \pm 0.7$, for $0.01 \leq m/(\mathrm{M}_\odot) \geq 0.08$;
$\alpha_1 = +1.3 \pm 0.5$, for $0.08 \leq m/(\mathrm{M}_\odot) \geq 0.5$;
$\alpha_2 = +2.3 \pm 0.3$, for $0.5 \leq m/(\mathrm{M}_\odot) \geq 1.00$;
$\alpha_3 = +2.3 \pm 0.7$, for $1.00 \leq m/(\mathrm{M}_\odot)$.

6.3.2 The Integrator

The choice of the integration scheme is essential for an N-body simulation, since it regulates the time-discretization for the solution of Eq.6.1 and it tells us how the numerical error δE scales with the time step δt. For a scheme of order k, the algorithmic error is proportional to the time step to the k-th power [35].

$$\delta E \propto \delta t^k \tag{6.6}$$

The advantage of high order scheme is the possibility to use longer time steps with the same accuracy of the lower-order schemes. This is why we decided to implement the *ph4* dynamical module, MPI-parallel block time step fourth-order Hermite direct N-body code with GPU support [35]:

- **fourth-order Hermite scheme** (see next paragraph)
- **Direct N-body code**: The *ph4* module uses additional parameters during the solution of Eq. 6.1, sometimes to reduce the time or the errors linked to the round-off. The computational expense is directly proportional to the number of particles in the simulation [35].
- **supported by GPU**: the most used acceleration hardware in N-body simulations is graphics processing unit (GPU), a tiny computer that when combined with others is very poweful. The substantial advantage of GPUs is that they are able to compute in a single operation the acceleration and its temporal derivative on many pairs of particles, therefore each force between a pair of bodies is independent of the other pairs. This implies that any change in the position and velocity can be updated independently of the other stars and simultaneously [20].

Hermite timestep scheme

The **fourth-order Hermite scheme** is an **explicit** method, implying that the state of the system at time $t + \Delta t$ depends only on the variables of the time step t [2] .

In the Hermite timestep scheme, each particle i is characterized by a timestep Δ_i and, at time t_i, its position x_i, velocity v_i, acceleration a_i and derivative of acceleration $\dot{a}_i$ (Makino and Aarseth, 1992 [17]).

It is a **predictor-evaluator-corrector** scheme and the integration steps are [17]:

1. Select particle i with a minimum value $t_i + \Delta t_i$ and set the global time t to be this minimum, $t_i + \Delta t_i$
2. Predict positions $\mathbf{x}_{p,j}$ and velocities $\mathbf{v}_{p,j}$ of all the particles at time t using the third order Taylor expansion starting from **x,v,a** and $\dot{\mathbf{a}}$:

$$\mathbf{x}_{p,j} = \frac{(t-t_j)^3}{6}\dot{\mathbf{a}}_j + \frac{(t-t_j)^2}{2}\mathbf{a}_j + (t-t_j)\mathbf{v}_j + \mathbf{x}_j \tag{6.7}$$

$$\mathbf{v}_{p,j} = \frac{(t-t_j)^2}{2}\dot{\mathbf{a}}_j + (t-t_j)\mathbf{a}_j + \mathbf{v}_j \tag{6.8}$$

   where j runs for all the particles of the set, including the particle i. The subscript p indicates that the obtained position and the velocity are not the definitive ones, but just the predicted ones [20].

[2] It is opposite of an implicit method, where the state of the system at time $t + \Delta t$ depends also on quantities that still need to be evaluated, because present in the next step. The solution is found by iterative steps, that imply an higher computational cost, even though they are more stable.

3. Compute the acceleration a_i and its derivative in time $\dot{a}_i$ at time t from the predicted positions $\mathbf{x}_{p,j}$ and velocities $\mathbf{v}_{p,j}$ with the following equations:

$$\mathbf{a}_i = \sum_j^N G m_j \frac{\mathbf{r}_{ij}}{(\mathbf{r}_{ij}^2 + \epsilon^2)^{3/2}} \tag{6.9}$$

$$\dot{\mathbf{a}}_i = \sum_j^N G m_j \left[\frac{\mathbf{v}_{ij}}{(\mathbf{r}_{ij}^2 + \epsilon^2)^{3/2}} + \frac{3(\mathbf{v}_{ij} \cdot \mathbf{r}_{ij})\mathbf{r}_{ij}}{(\mathbf{r}_{ij}^2 + \epsilon^2)^{5/2}} \right] \tag{6.10}$$

where ϵ is the softening parameter and

$$\mathbf{r}_{ij} = \mathbf{x}_{p,j} - \mathbf{x}_{p,i} \tag{6.11}$$

$$\mathbf{v}_{ij} = \mathbf{v}_{p,j} - \mathbf{v}_{p,i} \tag{6.12}$$

4. Use the third order Hermite interpolation polynomial:

$$\mathbf{a}_i(t) = \mathbf{a}_{0,i} + \Delta t \dot{\mathbf{a}}_{0,i} + \frac{(\Delta t)^2}{2}\mathbf{a}_{0,i}^{(2)} + \frac{(\Delta t)^3}{6}\mathbf{a}_{0,i}^{(3)} \tag{6.13}$$

where $\Delta t = t - t_i$, $\mathbf{a}_0$ and $\dot{\mathbf{a}}_0$ are the acceleration and its time derivative calculated at time t_i , $\mathbf{a}_{0,i}^{(2)}$ and $\mathbf{a}_{0,i}^{(3)}$ the derivative of second and third order in time of the acceleration at time t_i given by:

$$\mathbf{a}_{0,i}^{(2)} = \frac{-6(\mathbf{a}_{0,i} - \mathbf{a}_{1,i}) - \Delta t_i(4\dot{\mathbf{a}}_{0,i} + 2\dot{\mathbf{a}}_{1,i})}{\Delta t_i^2} \tag{6.14}$$

$$\mathbf{a}_{0,i}^{(3)} = \frac{12(\mathbf{a}_{0,i} - \mathbf{a}_{1,i}) + 6\Delta t_i(\dot{\mathbf{a}}_{0,i} + \dot{\mathbf{a}}_{1,i})}{\Delta t_i^3} \tag{6.15}$$

where $\mathbf{a}_{1,i}$ and $\dot{\mathbf{a}}_{1,i}$ are the acceleration and its derivative at time $t_i + \Delta t_i$.

Subsequently we correct the position and the velocity of the particle i using a fourth-order polynomial:

$$\mathbf{x}_i(t_i + \Delta t_i) = \mathbf{x}_{p,i} + \frac{\Delta t_i^4}{24}\mathbf{a}_{0,i}^{(2)} + \frac{(\Delta t_i)^5}{120}\mathbf{a}_{0,i}^{(3)} \tag{6.16}$$

$$\mathbf{v}(t + \Delta t_i) = \mathbf{v}_{p,i} + \frac{\Delta t_i^3}{6}\mathbf{a}_{0,i}^{(2)} + \frac{(\Delta t_i)^4}{24}\mathbf{a}_{0,i}^{(3)} \tag{6.17}$$

and then calculate the new timestep and update t_i.

One of the advantages in using a fourth-order Hermite scheme is that it is sufficiently high order to guarantee energy and angular momentum conservation to 10^{-5} or better [20].

Moreover, the predictor-corrector scheme is particularly convenient for the study of the stellar cluster, since the stellar positions and velocities are first predicted with lower level of accuracy and then they are corrected to higher accuracy starting from the prediction.

In particular, when we deal with stars that are not involved in collisional dynamics, the predictor step is enough for computing their position and velocities, therefore saving computational time. On the other hand, the stars that undergo to close encounters require more accuracy in the evaluation of their positions and velocities. Thus in this case we include the corrector step of our fourth-order scheme [20].

Accuracy of the model

One of the advantages of the N-body simulations are their deterministic results, thus always returning the same output starting from a specific set of initial conditions. This means that the initial conditions define just one trajectory in the phase space.

However, this path does not often coincide with the true phase space one: the exponential propagation of numerical errors in the temporal or spatial discretizations, in the integration scheme or in the round-off lead to the irreversibility of the calculations. As matter of fact, in N-body integrations the numerical errors can accumulate at each step so that the net error increases as the square root of the number of steps. Therefore the simulation is not time symmetric anymore [3]: in particular, with high-order numerical solvers the reduction of time steps can imply lack of precision due to the growth of the error introduced by round off (Portegies Zwart and Boekholt 2018 [39]).

On the other hand, with random errors and systematic effects, the accuracy of the final state of the simulation should be equivalent to the true one. This gives us confidence in implementing the N-body algorithms [35]. In our particular case, the long-term evolution of a star cluster, that takes into account the virialization, the mass segregation, the core collapse seems to not be essentially be influenced by the initial model and the integration technique. Therefore, we can rely on the overall predictions of the statistical properties of the cluster, but we should be careful in the analysis of the individual stellar orbits [35].

6.3.3 Coupling strategy

So far, we have two codes: one related to the galactic gravitational potential and another one linked to the force that the stars of the cluster exert on each other. These two effects are correlated and this is why we need to couple the two relative codes.

Generally, when a microscopic system (in our case the stellar cluster) dynamically interacts with a macroscopic one (the Milky Way), the first is the one that determines

[3] One way to solve this problem could be using integer numbers instead of floating ones, as proved in the 3-body simulation proposed by Portegies Zwart and Boekholt 2018 [39], but it does not resolve accurately and precisely the stellar encounters, which are fundamental for our simulation.

the time resolution and time step for the evolution of the system, while the second is responsible for consuming more computational time, memory capacity and communication bandwidth. In order to tackle this problem, sometimes one of the two systems is approximated with a semi-analytic model. In this case, it is possible to distinguish two methods [35]:

- **background field method**, that consists in replacing the macroscopic model with an approximated solution
- **sub-grid physics**, when the microscopic system is described by an approximated model

In our case, as seen in Sec. 6.2, we have reduced the galactic tidal field to an analytic potential in which the stars evolve, so we adopt the background field method.

In order to couple these two codes and simultaneously have a flexible and dynamic result, we use the **Bridge method**, that allows the user to control the degree of coupling between solvers and eventually create multiple bridges for the hierarchical coupling.

The first Bridge scheme was formulated by Fujii et al. 2007 [22] who realised a fully self-consistent N-body simulation of star cluster in the galactic potential field, an accurate time integration for star clusters and a fast time integration for the galactic field.

In more detail, the bridge scheme presents a direct and Hermite scheme for the internal integration of the star cluster with high accuracy, while the tree algorithm is used to modulate the interactions between the elements of the galaxy and between the cluster and the galaxy itself [22].

The Bridge code is based on a symplectic[4] integrator: the leapfrog scheme.

The Leapfrog scheme

The Hamilton equation is written as Poisson bracket operator [22]:

$$\frac{df}{dt} = \{f, H\} \tag{6.18}$$

where f is a function of time t.

Then it can be defined the differential evolution operator D_H:

$$D_H f := \{f, H\} \tag{6.19}$$

so the solution of Eq. 6.18 becomes:

$$f(t) = e^{tD_H} f(0) \tag{6.20}$$

An integration algorithm of the N-body simulation can be approximated to the expression in Eq. 6.20.

For instance, the second order leapfrog integrator is described as follows [22].

[4] it preserves phase-space volume and hence is time-reversible [35]

The expression of the Hamiltonian for a N-body system is :

$$H = \sum_{i}^{N} \frac{p_i^2}{2m_i} - \sum_{i<j}^{N} \frac{Gm_i m_j}{r_{ij}} \tag{6.21}$$

It is possible to separate the Hamiltonian into two components:

$$H_A = -\sum_{i<j}^{N} \frac{Gm_i m_j}{r_{ij}} \tag{6.22}$$

$$H_B = \sum_{i}^{N} \frac{p_i^2}{2m_i} \tag{6.23}$$

Then the formal solution of f from time t to time $t + \Delta t$ is:

$$f(t + \Delta t) = e^{\Delta t(A+B)} f(t) \tag{6.24}$$

where $a := D_{H_A}$ and $B := D_{H_B}$.
If the previous operator is Taylor-expanded, the result will be:

$$e^{\Delta t(A+B)} = \prod_{i=1}^{k} e^{a_i \Delta t A} e^{b_i \Delta t B} + O(\Delta t^{n+1}) \tag{6.25}$$

where $(ai, b_i)(i = 1,2...k)$ is a set of real numbers and n is an integer that represented the order of the integrator. In Eq. 6.25 the quantity $O(\Delta t^{n+1})$ is neglected, the equation becomes:

$$f'(t + \Delta t) = \prod_{i=1}^{k} e^{a_i \Delta t A} e^{b_i \Delta t B} f(t) \tag{6.26}$$

The Eq. 6.26 is a n-th order symplectic integrator.
Assuming that k=2, $a_1 = a_2 = \frac{1}{2}$ and $b_1 = 1, b_2 = 0$ and then n=2, the Eq.6.25 can be rewritten as:

$$e^{\Delta t(A+B)} = e^{\frac{1}{2}\Delta t A} e^{\Delta t B} e^{\frac{1}{2}\Delta t A} + O(\Delta t^3) \tag{6.27}$$

As a consequence, the time evolution is described by the following formula:

$$f'(t + \Delta t) = e^{\frac{1}{2}\Delta t A} e^{\Delta t B} e^{\frac{1}{2}\Delta t A} f(t) \tag{6.28}$$

The Eq. 6.28 is a second-order leapfrog scheme, that is equivalent to the equations:

$$\mathbf{v}_{\frac{1}{2}} = \mathbf{v}_0 + \frac{1}{2}\Delta t \mathbf{a}_0 \tag{6.29}$$

$$\mathbf{x}_1 = \mathbf{x}_0 + \Delta t \mathbf{v}_{\frac{1}{2}} \tag{6.30}$$

$$\mathbf{v}_1 = \mathbf{v}_0 + \frac{1}{2}\Delta t \mathbf{a}_1 \tag{6.31}$$

where the subscripts $0, \frac{1}{2}$ and 1 refer respectively to $t, t + \frac{1}{2}\Delta t, t + \Delta t$.
The leapfrog scheme can be syntetized as follows [22]:

1. compute the acceleration at time t $\mathbf{a}_0$, then update the velocity $\mathbf{v}_{\frac{1}{2}}$ described in Eq.6.29
2. update the position $\mathbf{x}_1$ using the computed velocity $\mathbf{v}_{\frac{1}{2}}$ using the Eq.6.30
3. calculate the acceleration at time $t + \Delta t$ $\mathbf{a}_1$ by using the computed position $\mathbf{x}_1$, and then update the velocity $\mathbf{v}_1$ in the Eq. 6.31
4. repeat step 1-3

Bridge method

As before, the Hamiltonian of the N-body system is divided into two components [22]:

$$H = H_\alpha + H_\beta \tag{6.32}$$

where H_α and H_β are defined as follows:

$$H_\alpha = -\sum_{i<j}^{N_G} \frac{G m_{G,i} m_{G,j}}{r_{ij}} - \sum_{i=1}^{N_G} \sum_{j=1}^{N_{SC}} \frac{G m_{G,i} m_{SC,j}}{r_{ij}} \tag{6.33}$$

$$H_\beta = -\sum_{i=1}^{N_G} \frac{p_{G,i}^2}{2m_{G,i}} + \sum_{i=1}^{N_{SC}} \frac{p_{SC,i}^2}{2m_{SC,i}} - \sum_{i<j}^{N_{SC}} \frac{G m_{SC,i} m_{SC,j}}{r_{ij}} \tag{6.34}$$

In Eq. 6.33 and 6.34, N_G and N_{SC} are respectively the number of galaxy particles and the one in the star cluster, H_α is the potential energy of the gravitational interactions between the galaxy particles and the cluster ones, H_β is the kinetic energy of all the particles and the potential energy of the cluster stars [22].

If H_α is replaced with H_A and H_β with H_B and these factors are substituted in the Eq.6.28:

$$f'(t + \Delta t) = e^{\frac{1}{2}\Delta t \alpha} e^{\Delta t \beta} e^{\frac{1}{2}\Delta t \alpha} f(t) \tag{6.35}$$

where, by definition, $\alpha := D_{H_\alpha}$ and $\beta := D_{H_\beta}$.

In order to properly develop the coupling, it is necessary to integrate the star cluster and then the galaxy particles.

On one hand, the integrator for the stellar cluster is based on a fourth-order Hermite scheme and is described by the equations:

$$\mathbf{v'}_{SC,0} = \mathbf{v}_{SC,0} + \frac{1}{2}\Delta t \mathbf{a}_{(G \to SC,0)} \tag{6.36}$$

$$\mathbf{x}_{SC,0} \to \text{Hermite scheme} \to \mathbf{x}_{SC,1} \tag{6.37}$$

$$\mathbf{v'}_{SC,0} \to \text{Hermite scheme} \to \mathbf{v'}_{SC,1} \tag{6.38}$$

$$\mathbf{v}_{SC,1} = \mathbf{v'}_{SC,1} + \frac{1}{2}\Delta t \mathbf{a}_{(G\to SC,1)} \tag{6.39}$$

where the subscripts the subscripts $0, \frac{1}{2}$ and 1 refer respectively to $t, t+\frac{1}{2}\Delta t, t+\Delta t$, G and SC stand for respectively the galaxy and the star cluster, $\mathbf{v'}_{SC,1}$ is the velocity at $t+\Delta t$ computed using the Hermite scheme.

On the other hand, for the galaxy it has been implemented the leapfrog integrator, that follows the scheme:

$$\mathbf{v}_{G,\frac{1}{2}} = \mathbf{v}_{G,0} + \frac{1}{2}\Delta t \mathbf{a}_{(All\to G,0)} \tag{6.40}$$

$$\mathbf{x}_{G,1} = \mathbf{x}_{G,0} + \Delta t \mathbf{v}_{G,\frac{1}{2}} \tag{6.41}$$

$$\mathbf{v}_{G,1} = \mathbf{v}_{G,\frac{1}{2}} + \frac{1}{2}\Delta t \mathbf{a}_{(All\to G,1)} \tag{6.42}$$

where $\mathbf{a}_{(All\to G,0)}$ represents the gravitational acceleration exerted from all particles (including star cluster particles) to the galaxy particle.

The Bridge model is a kick-drift-kick Verlet-leapfrog scheme that can be summarized as follows [35]:

1. firstly kick the cluster star velocities with time step $\frac{1}{2}\Delta t$ using accelerations due to the galaxy $\mathbf{a}_{(G\to SC,0)}$ (Eq.6.36);

   Then kick galaxy particle velocities with time step $\frac{1}{2}\Delta t$ using accelerations due to both galaxy and cluster $\mathbf{a}_{(All\to G,0)}$ (Eq.6.40)

2. Later update (drift) cluster positions $\mathbf{x}_{SC,1}$ and the kicked velocities $\mathbf{v}_{SC,1}$ with time step Δt, using the internal cluster integration scheme (the Hermite scheme) and kicked velocities (Eq.6.37 and Eq.6.38);

   then update galaxy particle positions $\mathbf{x}_{G,1}$ with time step Δt using kicked velocities(Eq. 6.41)

3. Finally recompute the accelerations $\mathbf{a}_{(G\to SC,1)}$ and $\mathbf{a}_{(All\to G,1)}$ and then update (kicking) all cluster and galaxy velocities, $\mathbf{v}_{SC,1}$ and $\mathbf{v}_{G,1}$, respectively (Eq. 6.39 and Eq.6.42)

4. Repeat steps 1-3

In our code, the implementation of Bridge gave us the result of a cluster that affects the galaxy and vice versa.

A schematic representation of the Bridge so far can be seen in Fig. 6.1.

Moreover, we know that the threading (or multiprocessing) is a function in Bridge often applied because the two bridge steps are intrinsically parallel and most of the computers allow the use of multiple core simultaneously, however in some computers (especially in the old ones) this threading is responsible for memory conflicts. Therefore we have decided to switch off the internal threading of the bridged codes by adding as argument in bridge: $use\_threading = False$ [35].

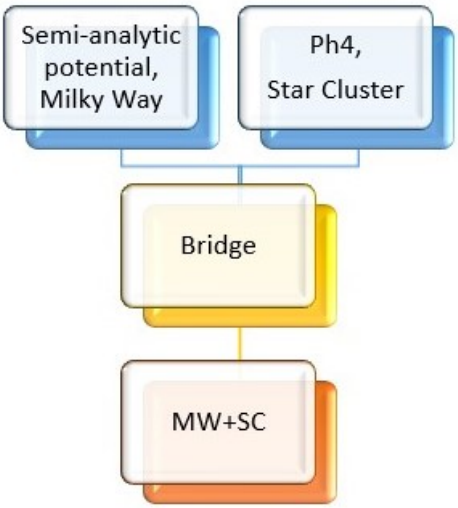

Figure 6.1: Schematic representation of Bridge: on top we have the N-body integrator *ph4* that regulates the interaction between the stars in the cluster and the semi-analytic solution for the Galactic potential. Then in the subsequent step these codes are coupled, leading to a simple bridge that integrates the system composed by Milky Way and Star Cluster.

Channels

A fundamental tool for the coupling strategy are the channels, specific MPI communication links that it is not necessary to restore every time. They allow the communication between different modules in a fast, efficient and clear way and they are independent of specific hardware and software implementations of inter-process communication [35].

In our code we have to deal with the stellar evolution and gravity integrator, so it is necessary to set three channels: one that links the data from stellar evolution code to the local python framework, one for the gravity solver to the framework and another one to copy the data from the framework to the gravity code [35].

6.3.4 Stellar Evolution model

The simulation of stellar evolution is by far more complicated than the gravitational force in the cluster. It involves hydrodynamics, nuclear reactions and modeling the interaction between matter and energy. Given the complexity of the phenomenon, it is necessary to apply some assumptions, taking into consideration mostly the macroscopic effects linked to the stellar evolution rather then the microscopic ones [35]. The most important approximations are that the stars are considered as **spherical symmetric** objects, in order to reduce the number of partial differential equations from three to one, so there is no stellar rotation, magnetic field and any type of motion that does not propagate in the radial direction [35].

According to the previous studies, the model built up on these assumptions approximates correctly the real stellar evolution to the first order [35].

There are two types of stellar codes solvers [35]:

- direct stellar evolution codes, the **Henyey models**, that describe the stars as 1D set of partial differential equations along the radial direction. They simulate the internal structure and include the atmosphere, the rotations and convective models.

- derived stellar evolution codes can be parametric and look-up. The **look-up parametric** codes are characterized by fitting formulae that represent each stage of the evolution. So we are able to retrieve temperature, luminosity and the radius of the stars from polynomials with free parameters as mass and metallicity. As output, the amount of internal parameters is limited with respect to the Henyey modes, but they are much faster.

A comparison between a direct code (MESA) and derived one (SeBa) is provided in Fig. 6.2. As we can see, the red giant branch is more developed in the SeBa code and the MESA one lacks of the white dwarf stage and is more time consuming [35].

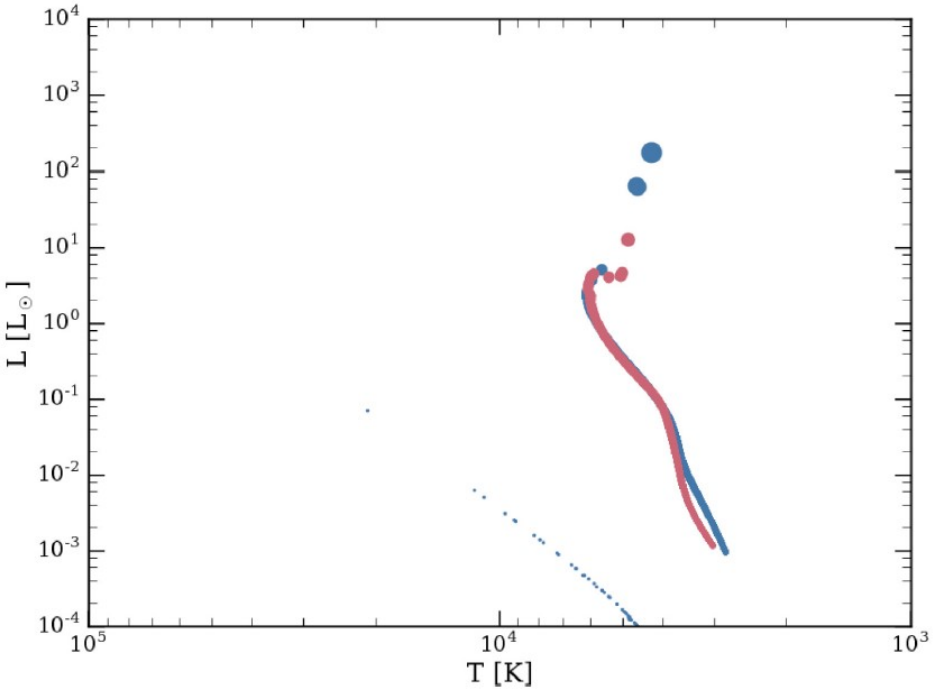

Figure 6.2: This is the graphical representation of the Hertzsprung-Russel diagram of 3000 stars. The evolution has been protracted to 4.5 Gyr and the initial masses range between 0.1 $M_\odot$ and 100 $M_\odot$. The blue HR is the SeBa HR, while the red one is the MESA one [35].

6.3.5 SeBa code

We couple the *ph4* module with the SeBa package for the stellar evolution, drawn from Starlab's kira integrator (Portegies Zwart et al. 2001 [30]). It is based on fitting formulas with approximations for every small variation in mass and in time.

The SeBa package can be used for the evolution of a single star, of two stars simultaneously or for a cluster of stars, as in our case.

The evolution of the stars is modeled via the time dependent mass-radius relations for solar metallicities given by Eggleton et al., 1989 [11] with corrections by Eggleton et al. 1990 [10] and Tout et al. 1997 [36]. These equations provide the radius of a star as a function of time and the star's initial mass on the zero-age main-sequence ZAMS. The mass of the stellar core and the rate of mass loss via a stellar wind are fundamental for the binary evolution and the stellar cluster one, so it has been included the implementation by Portegies Zwart and Verbunt,1996 [29]. In the code the stellar types are identified with the values reported in Tab. 6.2 [30]:

Interface with kira

The interaction between stellar evolution the dynamical one of the cluster are difficult to couple. The orbit of the stars are described in Sec. 6.3.

We can define a stellar evolution time step as the time taken for the star to evolve from the start of one evolutionary stage to the next. The stellar and binary evolution is updated at fixed intervals (every 1/64 of a crossing time, typically a few thousand years) [30].

After each stellar evolution step, there is an update on the stellar radii of the stars for describing their trajectories. However, this does not happen for the mass, since it would imply the recalculation of the accelerations of the stars in the cluster. The change in mass is notified only when the mass of any star has changed by more than 1%, or if the orbital parameters, as semi-major axis, eccentricity, total mass or mass ratio of any binary has changed by more than 0.1% [30].

Accuracy of the model

The accuracy of SeBa code and the evolutionary stages are hard to validate, because we cannot observe the phases which every star goes through starting from their birth to death. Everything we are able to measure are the luminosity (that is an indicator of the mass) and the color of the star (that is an index of the effective temperature of the star), their atmospheric composition, pulsation and the internal structure (from asteroseismology).

To validate the model, the stellar evolution tracks have been successfully compared with the star cluster isochrones, conferming the reliability of the stellar models.

Moreover, it has been compared **four stellar evolution codes** available in AMUSE with the well-known solar position in the HR diagram (taken from Cox 2000 [9]) and the result can be seen in Fig. 6.3. For each model it has been computed the star (points) with the luminosity L and the temperature T closer to the Sun (yellow) and it is evident that none of the models perfectly fits the Sun: the error bar in the measure of the

Ref. Number	Stellar Type	Brief Description
0	proto star	Non hydrogen burning stars on the Hyashi track
1	planet	Various types, such as gas giants, etc.; also includes moons.
2	brown dwarf	Star with mass below the hydrogen-burning limit.
3	main sequence	Core hydrogen burning star.
4	Hypergiant	Massive (m>25Msun) post main sequence star with enormous mass-loss rate in a stage of evolution prior to becoming a Wolf-Rayet star.
5	Hertzsprung gap	Rapid evolution from the Terminal-age main sequence to the point when the hydrogen-depleted core exceeds the Schonberg-Chandrasekhar limit.
6	sub giant	Hydrogen shell burning star.
7	horizontal branch	Helium core burning star.
8	supergiant	Double shell burning star.
9-10-11	Helium star	Helium core of a stripped giant, the result of mass transfer in a binary. Subdivided into carbon core (9), helium dwarf (10) and helium giant (11).
12	carbon dwarf	A carbon star is a star with carbon to oxygen ratio (C/O) grater than one
13	Helium white dwarf	Stars of very low massare unable to fuse helium; hence, a helium white dwarf may form by mass loss in binary systems.
14	oxygen dwarf	A carbon star is a star with carbon to oxygen ratio (C/O) smaller than one
15	Thorne-Zytkow	Shell burning hydrogen envelope with neutron star core.
16	X-ray pulsar	a pulsar is highly magnetized rotating neutron star that emits beams of electromagnetic radiation out of its magnetic poles.It is an X-ray sources displaying strict periodic variations in X-ray intensity.
17	radio pulsar	pulsar that emits in radio wavelength
18	inert neutron star	neutron star with mass m $< 2\ M_{\odot}$
19	black hole	Star with radius smaller than the event horizon. The result of evolution of massive (m>25$M_{\odot}$) star or collapsed neutron star.
20	disintegrated	Result of Carbon detonation to Type Ia supernova.

Table 6.2: List of Stellar type in SeBa code. In the first column we have the reference number of the stellar type, the second one presents the name of the stellar type and the third one briefly describes it

solar properties is still smaller than the difference from the most likely solar star in the simulations.

Furthermore, the relative difference between the models is not significant, but must not be underestimated, since some phenomena (as the stellar wind) do not only depend in the dynamics of the cluster but also on the stellar evolution.

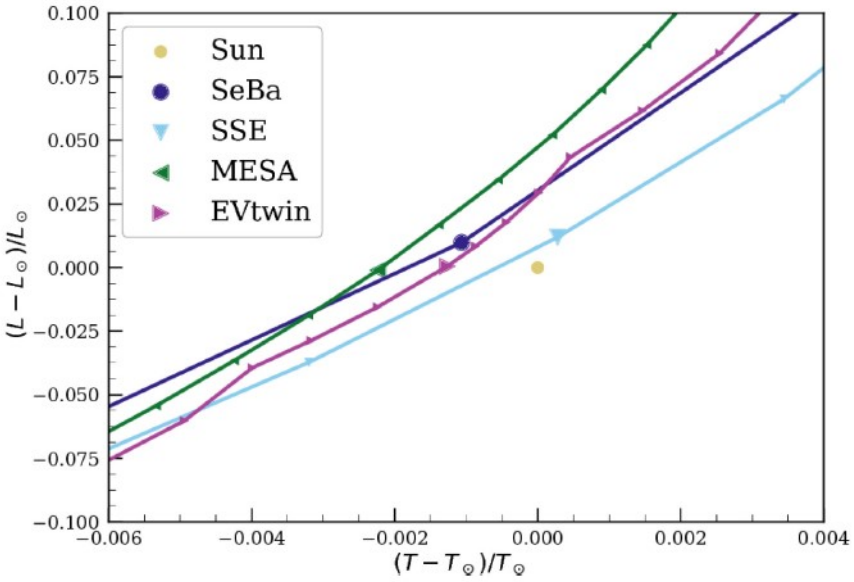

Figure 6.3: Comparison between the HR obtained with four stellar codes available in AMUSE and the solar data. In particular, the initial conditions for the simulations are a solar metallicity star with an initial mass 1 $M_\odot$,starting from an initial time of 4.0 Gyr and it evolves for 1.2 Gyr. [35]

In addition, stellar evolution can affect the gravitational one by influencing the behaviour of the binaries. The **binary** trajectories are defined not only by the random encounters, but also by the stellar evolutionary stage, and the coupled stars are responsible for the increasing of the computational time of the N-body code and for the accumulation of integration and round-off errors.

6.4 Asteroids

The life-bearing asteroids are the true protagonists of our simulation. They are the mechanisms for dispersal of microbiological organisms through space.

6.4.1 Initial conditions

In our simulation the asteroids are represented as spherically symmetric particles with null spatial extension and mass-less, in order to drastically reduce the computational time of our simulation.
Each asteroid is launched from every Sun-like star of mass between 0.9 and 1.1 $M_\odot$ on the

main sequence at a distance of 1000 AU from the star: we do not simulate the trajectory and its perturbation inside the solar systems, but we directly create a **uniform sphere** of asteroids that expands outside the planetary system. The reason behind this decision resides in the numerous previous studies that have provided huge amount of data on the asteroids ejection (e.g. Worth et al.2013 [37]), allowing us to save computational time for the integration of the asteroids in the stellar cluster.

Ejection speed distribution

The biologically active rocks must firstly be ejected from the planetary surface. For example, the escape velocity from the Earth-like planet is around $\sim 11 km/s$. However, the asteroid has also to escape from from the orbital location within the system and the necessary escape velocity is $\sim 42 km/s$ (Adams et a. 2022 [5]).

From the moment the asteroids are launched from the Eart-like planet, over the subsequent orbits they will undergo the influence of the **planets**, that will perturb their trajectory and on average only the 5% of the ejected asteroids will reach the outer part of the planetary system [37].

If the rock expulsion is due to close encounter, then the distribution of the ejection speeds can be approximated to the following formula [5]:

$$F(v) = \frac{4\frac{v}{v_p}}{(1+\frac{v^2}{v_p^2})^3} \tag{6.43}$$

where v_p is a velocity scale that depends on the location of the planet and on the extension of the gravitational potential exerted by the parent star and is described by the equation [5]:

$$v_p = \left(\frac{GM_\odot}{a_p}\right)^{\frac{1}{2}} \tag{6.44}$$

where a_p is the semi-major axis of the planet orbit. It is important to highlight that the planet that is responsible for the ejection of the rock in the outer space is not necessarily the habitable one where the asteroid comes from. For instance, most of the asteroids that originated from the Earth entered in resonance with Saturn and Jupiter and eventually were launched outside due to the perturbation from the two giant planets.

The Eq. 6.43 is typical of the asteroid leaving the stellar system, but in the **interstellar region** they experience numerous and distant encounters that will affect their distribution. In particular, in the cluster environment the stars approach a Maxwellian distribution with dispersion $\sigma \sim 1 km/s$ (Lada and Lada 2003 [19]) and the rocky bodies end up with the same distribution (Fig. 6.4).

Ejection time

To study the dynamical evolution of the asteroids, we generated three sets of simulations, in which all the Sun-like stars eject asteroids at different time from the birth of the cluster.

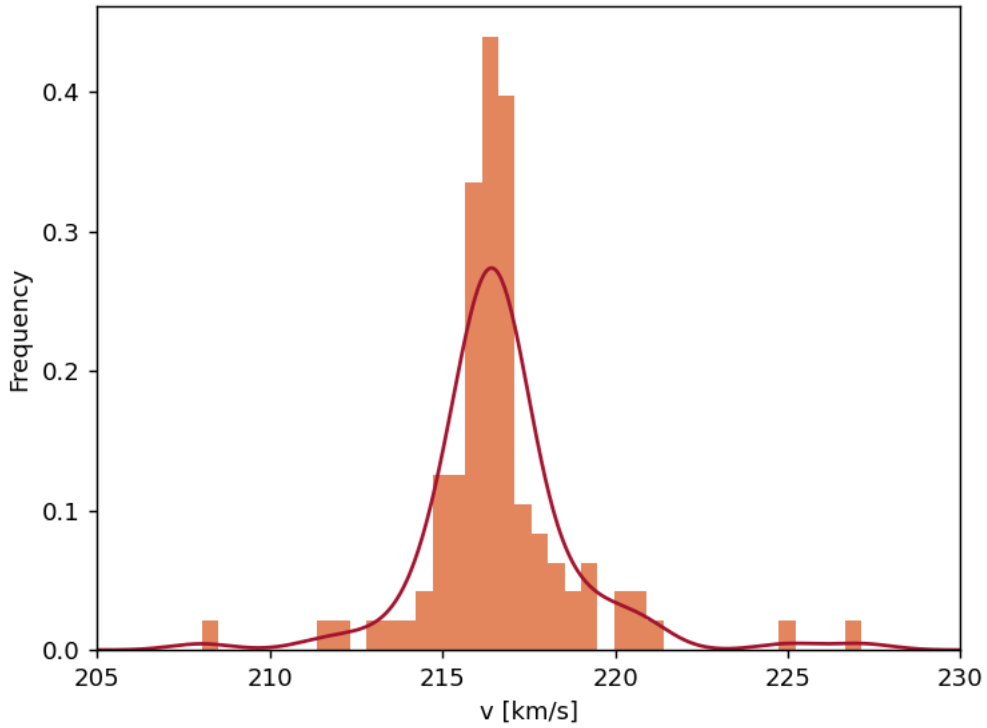

Figure 6.4: Velocity distribution of the asteroids at time 5 Myrs from the moment of the first ejection. The continuous line is the Kernel Density Estimation of the velocity.

On one hand, the asteroids, in order to be biologically active, must have been ejected from a planet that already presents life forms on its surface. We know that the first evidence of life on Earth appeared around 700-900 Myr after the birth of the cluster where Sun probably originated (e.g. Noffke et al. 2013 [27] and Nishizawa et al. 2005 [38]).

So we assume that the planet that launches the asteroids has been through the same biological evolution as the Earth, therefore fix the launching time at 900 Myr. We refer at this set as the '**delayed**' one.

On the other hand, we do not know the origin nor the primordial evolution of the first fossils discovered on the Earth, and we cannot ignore the possibility that they may have been originated from another planet and then they cross fertilized the Earth. In this case, we set the launching clock at 500 Myrs (the '**intermediate**' simulation) and at 250 Myr from the birth of the cluster ('**primordial**' one), so that the asteroids have enough time to being ejected from the parental planet, escape from their planetary system, travel in the interstellar region and then encounter with a solar system that resembles ours and fertilize the habitable planet.

Regarding the temporal interval of the launch of *soli lapides*, Worth et al. [37] found that the rate of ejection of asteroids from an Earth-like planet out of the solar system declines after 10 and 15 Myr. Therefore, in our simulation we launch the asteroids in a time interval of 10 Myrs, after which the total number of ejected asteroids remains constant (Fig. 6.5).

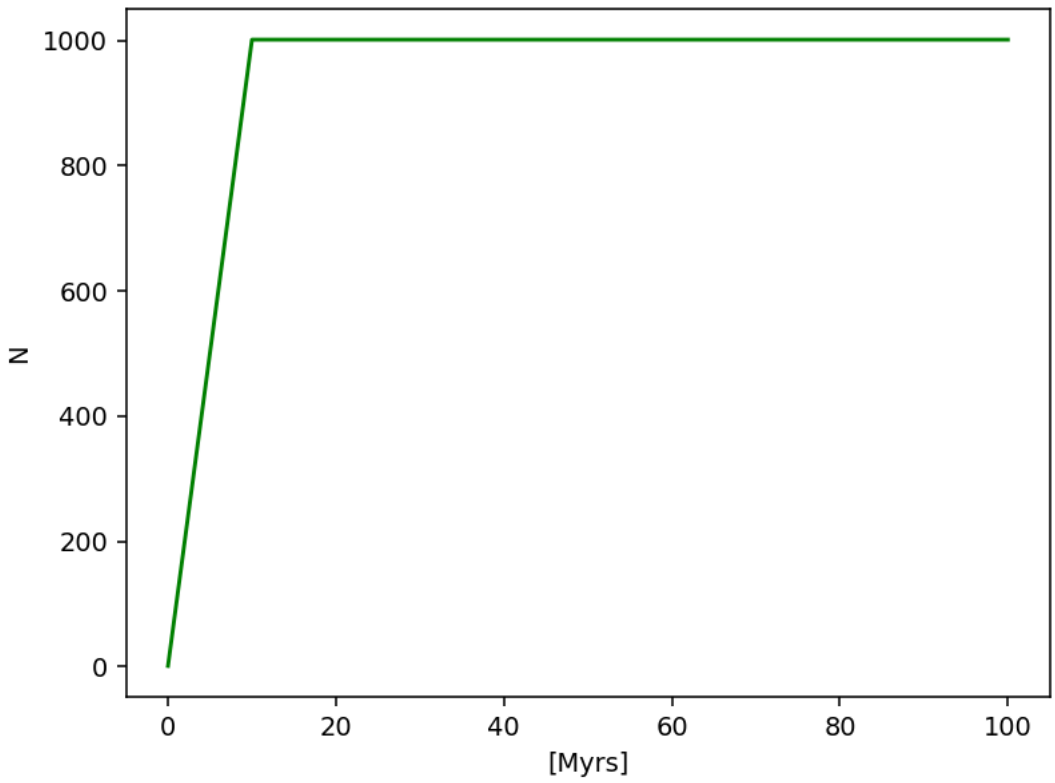

Figure 6.5: Representation of the number of asteroids launched from a Sun-like star and evolving in time. The asteroids are launched in the first 10 Myrs and then the rate of ejection is negligible ([37])

6.4.2 Hierarchical Bridge

At this stage, our simulation is characterized by the Bridge scheme that couples the *ph4* code for the N-body simulation of the cluster and the semi-analytic code for the gravitational potential of the Milky way that acts on the cluster (Fig.6.1).

The addition of the asteroids, even though we have applied some approximations, hugely increases the complexity and the computational time of the simulation.

In order to render the code reasonably fast, we approximate the particles as mass-less points (as mentioned before) and at each step their position is simply updated by adding

to its original value the measure $v\delta t$, where v is its position and δt the time step.

We implemented the **Hierarchical Bridge**, that, applied to our study, consists in two nested bridges. Firstly we couple the N-body integrator *ph4* that regulates the interaction between the stars in the cluster with the drift without gravity of the asteroids. In a subsequent step the bridge for realizing the interaction between rocks and stars is again bridged with the semi-analytic solution for the Galactic potential(Fig.6.6), leading to a simple composite bridge that integrates the entire system.

The implementation of the hierarchical bridge guarantees considerable flexibility that may compensate for possible loss of performance in many circumstances. For instance, in a simulation of codes that require intense computational performances, the overhead of the hierarchical bridge strategy is typically not more than a few percent.

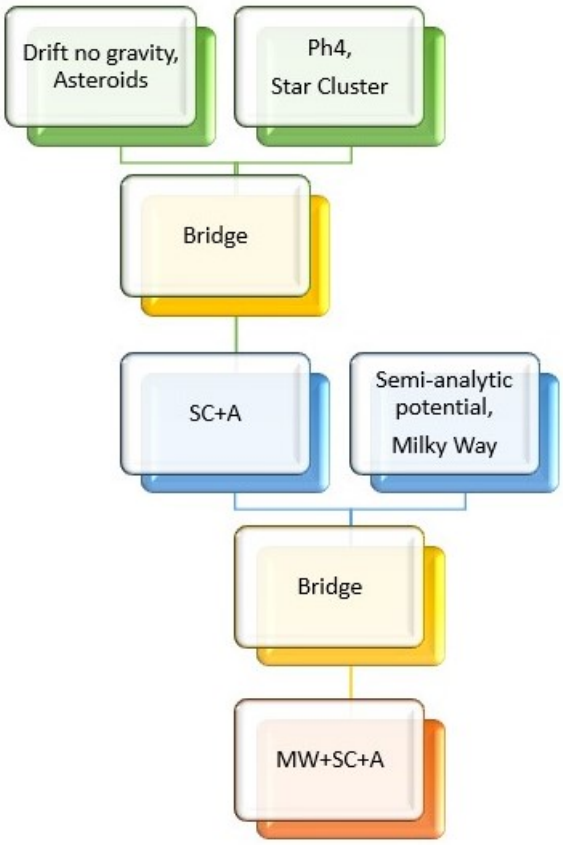

Figure 6.6: Schematic representation of the Hierarchical Bridge: on top we have the N-body integrator *ph4* that regulates the interaction between the stars in the cluster and the drift-without-gravity code for the asteroids. Then in the subsequent step these codes are couples. In the following stage there is the bridge for realizing the interaction between rocks and stars and the semi-analytic solution for the Galactic potential(Fig.6.6). Both of them are bridged (fourth step), leading to a simple composite bridge that integrates the entire system: Milky Way, Star Cluster and Asteroids.

Accuracy of the model

The hierarchical bridge is a procedure of which we do not have any formal confirmation of the validity of its result. However, the resolution and the convergence test give us further constrains on the reliability and accuracy of the method [35]. As a consequence, we believe in the suitability of the code for our scientific purposes.

Chapter 7

Results

The simulation consists in a star cluster that encloses 56 Sun-like stars, each of them responsible for the ejection of 1000 asteroids at different times from the birth of the cluster for 100 Myr (see Sub-sec. 6.4.1).

At the moment of the asteroids ejection, the stellar cluster is already dissolving: the Galactic tidal field is responsible the progressive disruption of the cluster, that assumes an elongated shape that lengthens as the cluster evolves.

We perform two types of analysis on the evolution of the asteroids:

- **Kernel Density Estimation**, that is the process of estimating an unknown probability density function using a kernel function. In our case, we use the Gaussian function as kernel [2].
- **Bound Orbits**: for each star, we consider the closest asteroid and then we check whether its orbit is bound or not.

Moreover, we adopt two different points of view:

- **Single star point of view**: we analyze the dynamical evolution and cross fertilization of the asteroids coming from just one of the Sun-like stars, neglecting all the other asteroids. We repeat it for every sender star in order to have a statistical measure of the lithopanspermia;
- **Global point of view**: we study the possibility of seeding the young cluster through all the asteroids in the simulation, making no distinction among the original planetary systems they come from.

7.1 Kernel Density Estimation

The Kernel Density Estimation is a mathematical process of estimating the probability density function of a random variable. The aim of this estimation is to infer the characteristics of a population, based on a finite set of data [3].

This type of analysis is also called **data smoothing problem** and is often used in signal processing and data science, since it is a powerful way to estimate probability density [3].

As a result, the KDE creates a smooth curve given a set of random data or can also be used to generate points that only appear to have come from a specific sample set. This feature finds particular application in numerical simulations and in object modeling [3].

7.1.1 How does it work?

The Kernel Density Estimation works by going through the following steps [3]:

1. plot out the data and begin to create a curve of the distribution
2. calculate the curve by weighing the distance of all the points in each specific location along the distribution
3. If there are more points grouped locally, the estimation is higher as the probability of seeing a point at that location increases.

The **kernel function** $K(u)$ is the specific mechanism used to weigh the points across the data set and in our case we choose the Gaussian function. The kernel function typically exhibits the following properties [2]:

- symmetry:
$$K(u) = K(-u) \tag{7.1}$$
- normalization:
$$\int_{-\infty}^{\infty} K(u)du = 1 \tag{7.2}$$
- monotonically decrease:
$$K'(u) < 0 \quad \text{for} \quad u > 0 \tag{7.3}$$

Tweaking the bandwidth and the amplitude of the kernel function, the shape and the size of the estimate can significantly change [2].

The **bandwidth** of the kernel is responsible for the modification of the shape. A too small bandwidth limits the scope of the function and makes the estimated curve look rough and jagged [2].

7.1.2 Single star point of view

A typical KDE can be found in Figs. 7.1 and 7.2, where we have the projection of the density distribution of the asteroids.

More in detail, in Fig.7.3 we can see the density distribution of the asteroids (green contours) ejected from the Sun-like star (yellow star), and it decreases as we go further from the star.

The peak of density distribution of the asteroids monotonically decreases over time (Fig.7.4) and has always the highest value in the first 1-2 Myr after the launch in all

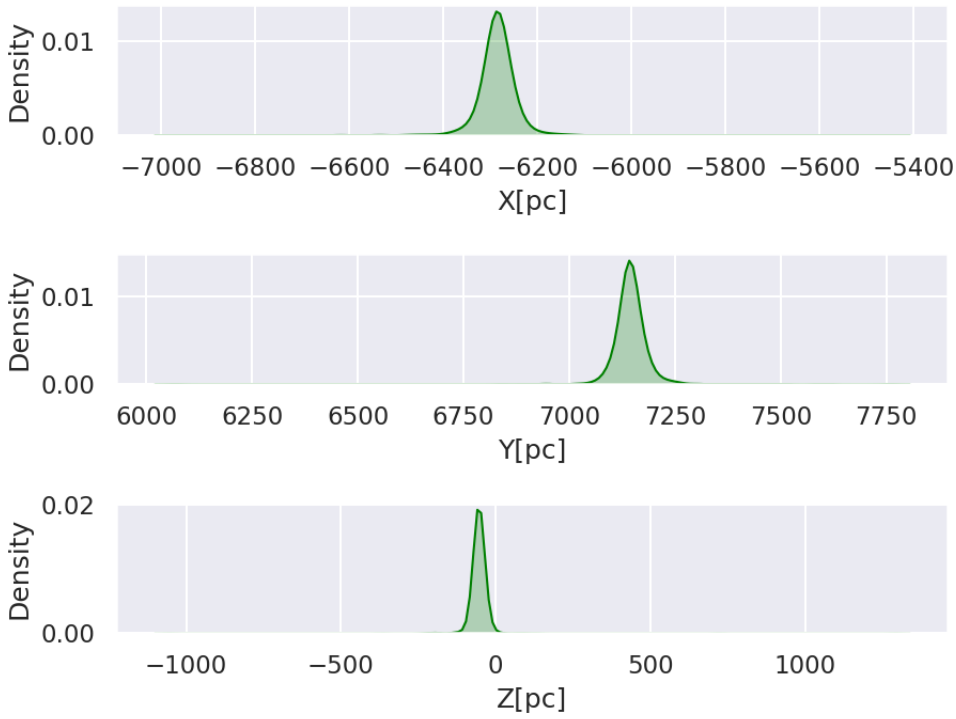

Figure 7.1: Projection of the KDE of the asteroids along the x, y, and z axis

the three simulations: the *primordial*, the *intermediate* and the *delayed* one, so when the ejection of the asteroids occurred at 250 Myr, 500 Myr and 950 Myr after the birth of the cluster, respectively.

This has important consequences on our results, since the decrease in the asteroids density over time implies that the receiving habitable planetary systems must be the **closest possible** to the parental star of the asteroids since the **first million years** from the ejections, in order to have a higher probability to be germinated.

In addition, the green color-bar in Fig.7.3 accounts for the value of the KDE computed on the space parameter of the stars. In particular, the highest values of the KDE are assigned to the stars that are closer to the region where the asteroids are more concentrated: the KDE is an index of the number of asteroids that surround the star, or in other words the likelihood that a star can be polluted by biologically active rocks.

7.1.3 Case I: far receiving planetary system

In Fig. 7.5, we can see the comparison between 4 snapshots at time 1, 5, 10, 15 Myr after the launch of the asteroids, respectively.

In the upper left part, the asteroids are not so numerous and they are quite concentrated close to their parent star, as we can see in the green density distribution of the

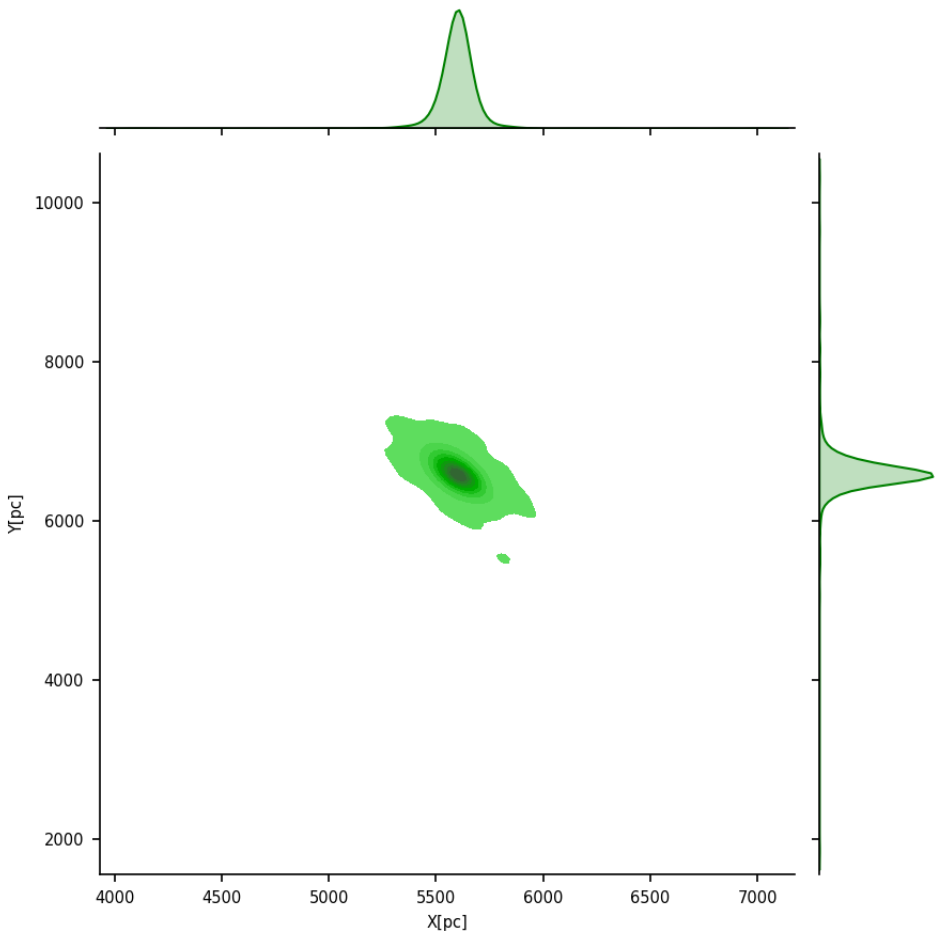

Figure 7.2: The two marginal panels show the projection along x and y axis of the KDE of the asteroids.The central panel shows its 2D representation.

rocky bodies.

The nearest star that can be polluted is the red one, which is at a distance 7 pc from the parent Sun-like star and, most importantly, far away from the asteroids. Therefore, the red star has a very low probability to be germinated, as we can see from the relative KDE value $\sim 10^{-18}$.

At time 5 Myr after the ejection (upper right image in Fig. 7.5), more asteroids have been launched, spreading out in the cluster and reaching more stars. In this case, the receiving planetary systems are well within the green distribution of the asteroids and particularly in the regions of higher concentration of asteroids. This implies that the stars in this area have a high probability to be polluted and the KDE has higher values with respect to the one at 1 Myr from the launch.

In the lower left image, the asteroids have been launched from 10 Myr. From this time

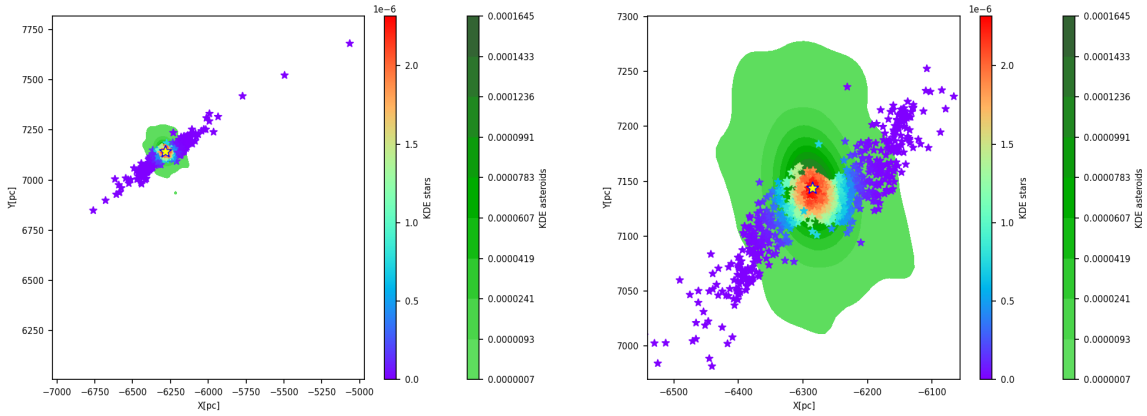

Figure 7.3: Left: star cluster representation with the density distribution of the asteroids (in green) coming from just one Sun-like star (in yellow). The other stars colour map represents the likelihood of the stars being polluted by the asteroid. The higher is the value of the KDE (towards red), the higher are the chances of cross fertilization. In this case, we adopt the single stellar point of view.
Right: zoom-in of the left-hand panel around the Sun-like star

.

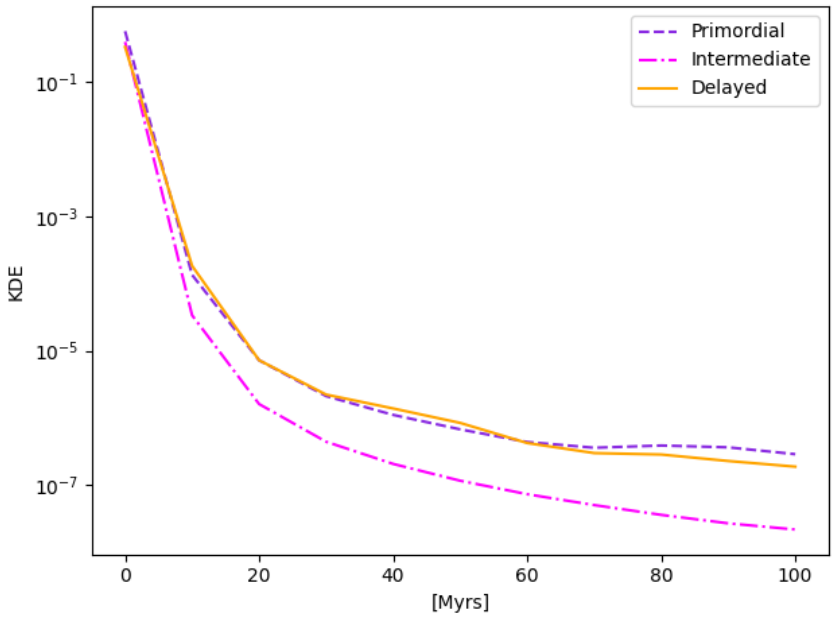

Figure 7.4: Evolution of the peak of the density distribution of the asteroids. The violet, pink and orange lines show the *primordial*, *intermediate* and *delayed* model, respectively

on the number of rocky bodies will be roughly constant and their spatial distribution in the cluster has increased even more.

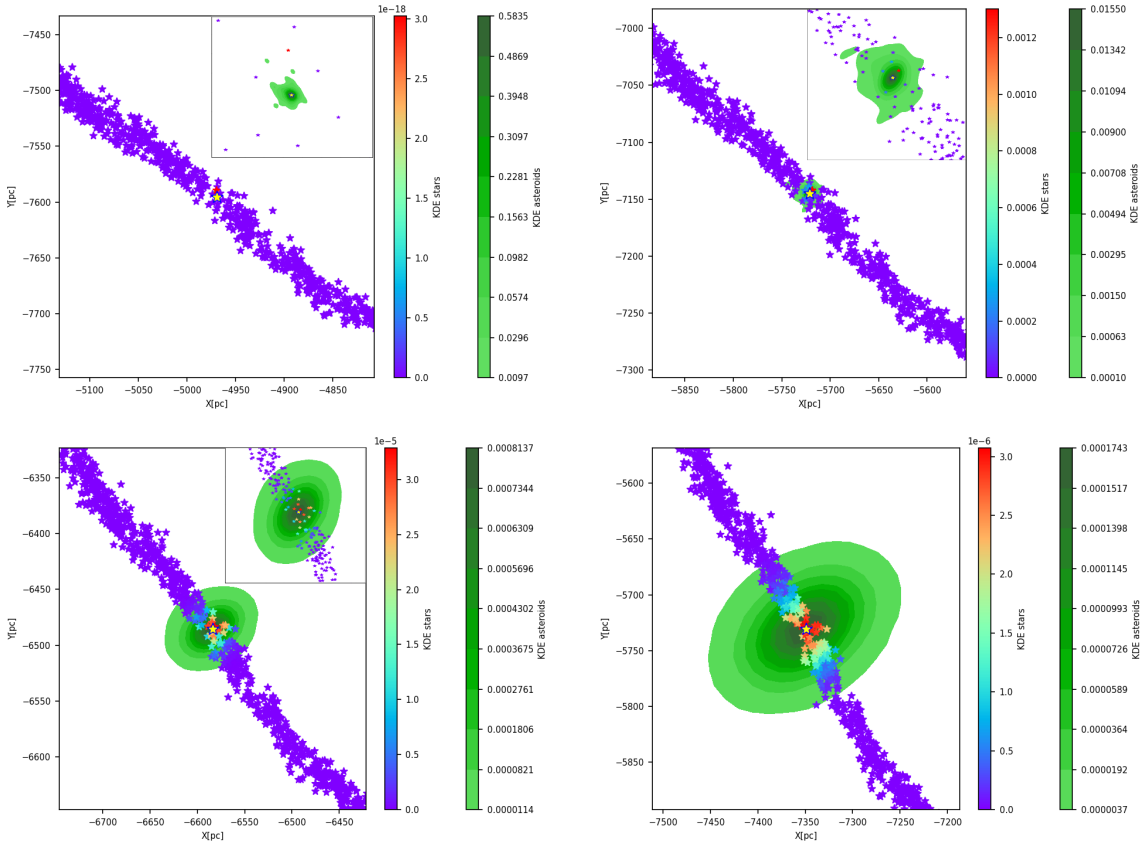

Figure 7.5: Time comparison of the KDE of the asteroids coming from the Sun-like star *s27* (yellow star at the center of the boxes), in the *delayed* simulation. From the upper left to the bottom right panel: the time is 1, 5, 10 and 15 Myr after the launch of the asteroids. In each panel, the green contours show the KDE of the asteroids, while the star symbols and the rainbow colour map show the KDE of the stars. In each panel, the inset is a zoom in of the central 50 pc around the parent star.

As a consequence, the number of stars that can be germinated has grown, but the number of asteroids surrounding each star issmaller (the asteroids decrease their density distribution over time, Fig. 7.4).

This decrease in the KDE maximum value is even more enhanced after 15 Myr from the launch of the asteroids: the rocky bodies will be even more spread out, reaching the outer regions of the cluster, but the number of possible polluters per each star will be much lower.

This concept can be visualized with the time evolution of the peak of the KDE over the time for the three sets of simulations (Fig. 7.6).

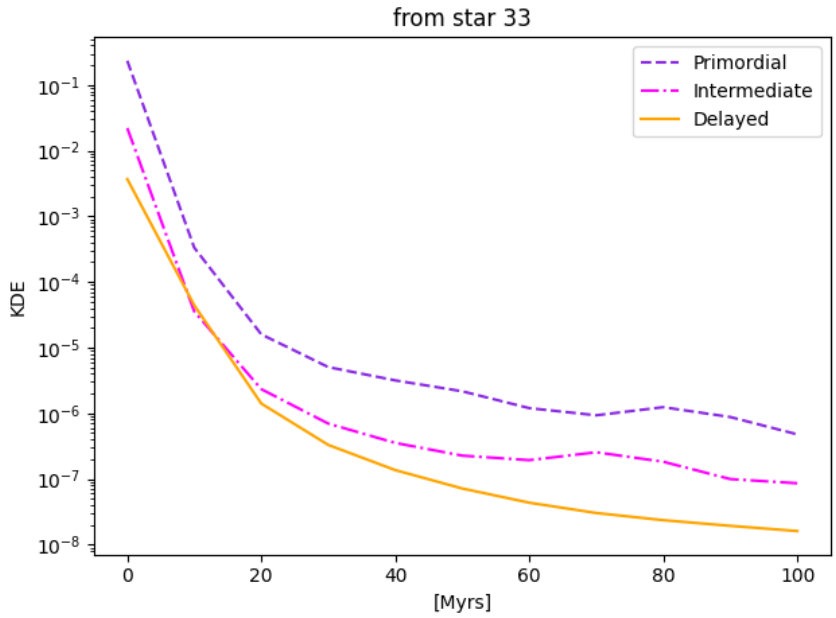

Figure 7.6: Evolution of the peak of the KDE of the asteroids coming from the Sun-like star *s33*. The colours and line types are the same as in Figure 7.4

.

7.1.4 Case II: close receiving star

As before, in Fig. 7.7, we have four time snapshots at time 1, 5, 10, 15 Myr after the launch of the asteroids, respectively.

In the upper left part, few asteroids have been launched from their parent star and their density distribution is represented by the green profile.

The star with the highest probability to be germinated is the red one. It is located at a distance 4 pc from the parent Sun-like star and so well within the region of the cluster dominated by the asteroids: the red star has a very high probability to be polluted since the beginning of the ejection, as it is inside the area where the asteroids are highly concentrated. Therefore, the KDE values are very high since the first $1-2$ Myr after the launch of the polluters.

As we go further in time, from 5 to 15 Myr after the escape of the asteroids from their parent planetary system, more asteroids have been launched, spreading out in the cluster and reaching more stars.

However, even though the number of stars that are close to the asteroids increases over time, the rate of asteroids around each star is highly reduced, since the density distribution of the rocky bodies decreases over time (Fig. 7.4).

Therefore, our KDE will have lower values as we go further in time and this concept can be visualized with the time evolution of the peak of the KDE (Fig. 7.8)

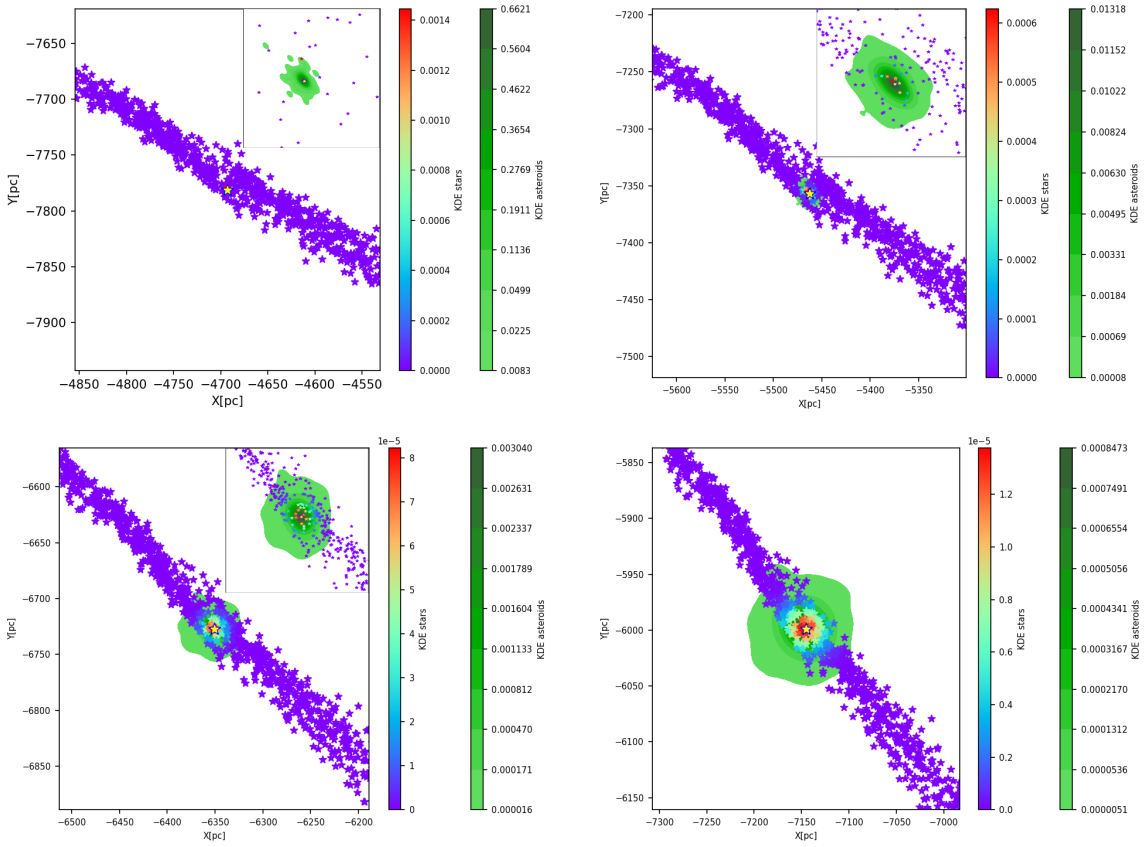

Figure 7.7: Temporal comparison of the KDE of the asteroids coming from the star *s15*, in the *delayed* simulation. In the upper left panel, we have a snapshot at time 1 Myr after the launch of the asteroids, with a zoom in the region of the Sun-like star that ejects the asteroids. In the upper right image, the representation of the cluster and the relative KDE at time 5 Myr after the ejection. At the bottom, from left to right, we have the plot of the KDE at time 10 and 15 Myr after the launch, respectively.

7.1.5 KDE evolution in the primordial, intermediate and delayed case

We analyze the evolution of the asteroids from the single point of view for the three types of simulations already mentioned: the **primordial**, the **intermediate** and the **delayed** one.

In the three sets of simulations, if we measure the change of the peak of the KDE over time, we obtain the following results:

1. 55.36% of the cases present the peak in the first 1-2 Myr for all the three models (Fig.7.6).

2. in 21,43% of the cases the peak is in the first $1-2$ Myr in the *primordial* and *intermediate* simulation, and at 10 Myr in the *delayed* simulation (Fig.7.9).

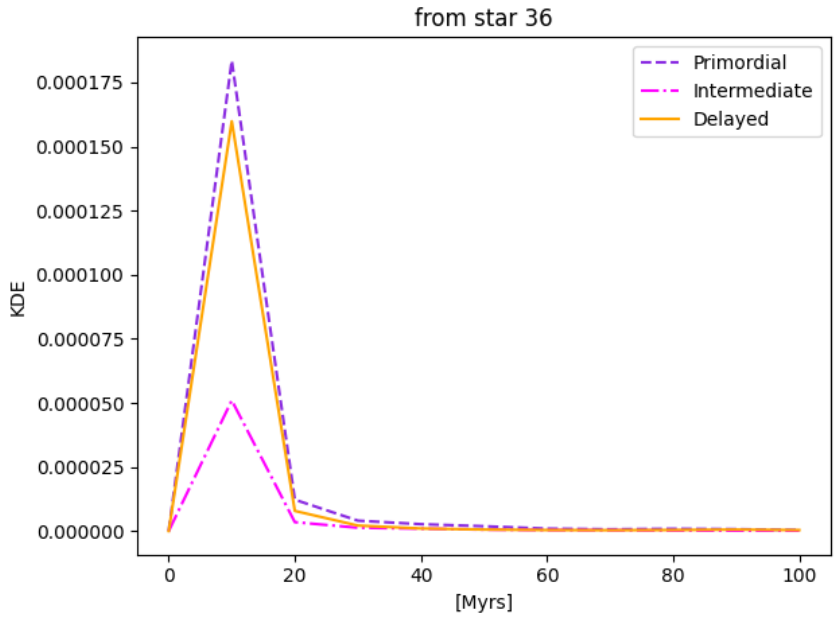

Figure 7.8: Evolution of the peak of the KDE of the asteroids coming from the Sun-like star *s36*. The colours and line types are the same as in Figure 7.4.

3. in 5,35 % of the cases the peak is at 10 Myr for all the three simulations (Fig.7.8).
4. if we compare for each star the KDEs of the **primordial, intermediate and delayed** simulations, 90,9% of the starshave the highest value of the KDE peak in the **primordial** simulation.

Given these results, we can infer from point 1 that it is more probable that the asteroids are transferred to another planetary system as soon as they are launched, increasing the probability of the microorganisms survival in the interstellar region and of the colonization on the receiving habitable planets.

From point 4 we deduce that the **earlier** the asteroid have been launched during the evolution of the cluster, earlier is the **peak** in the likelihood of the cross fertilization. As matter of fact, an asteroid has more chances to pollute other stars if launched at 250 Myr from the birth of the cluster (*primordial evolution*).

This could be explained with the **conformation of the cluster**: in the *primordial* model the asteroids are launched at 250 Myr, so when the stellar density is higher and therefore it is more likely that the asteroids are close to other stars than the parental one; on the other hand, as we progress in time in the launch the asteroids, the cluster is way more dissolved and the stars less crowded, leading to an improbable pollution.

This implies that the **Galactic tidal field** has a fundamental role in the cross fertilization: it is responsible for the dissolution of the star cluster, so the relative distance between the stars decreases, increasing the distance between stars and asteroids.

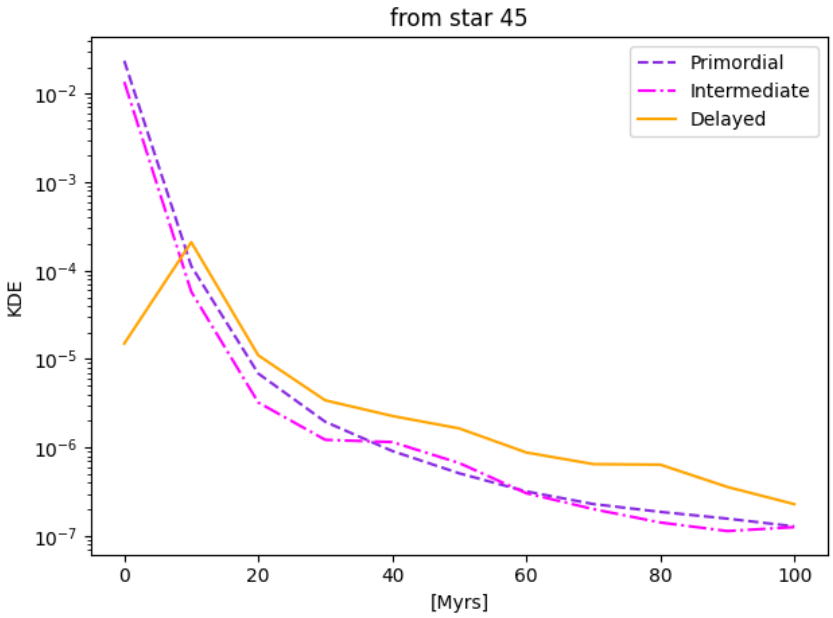

Figure 7.9: Evolution of the peak of the KDE of the asteroids coming from the Sun-like star *s45*. The colours and line types are the same as in Figure7.4.

7.1.6 The role of the initial relative distance

In addition, it is important to understand what is the main difference between the first case (Sec. 7.1.3) and the second one (Sec. 7.1.4). We found that the reason of this difference is the **relative distance** between the stars at the moment of the launch of the asteroids. From our analysis, there is a typical threshold of $5-6$ **pc**: the majority of Sun-like stars have higher probabilities to cross fertilize other planetary systems in the first $1-2$ Myr from the launch if they are surrounded by receiving stars at an initial distance less than $5-6$ **pc**.

On the other hand, if the minimum distance of the stars from the Sun is higher than this threshold, then they will be too far away from the asteroids at $1-2$ Myr after the ejection. Therefore, the maximum probability that the stars are polluted occurs at around $5-10$ Myr, when the asteroids are expanded enough to reach the stars (Fig.7.5).

7.1.7 Global point of view

Instead of analysing every time the dynamical evolution of the asteroids coming from a single star, we conduct a study on all the life-bearing rocks that travel in the cluster and may be captured by a planetary system.

Therefore, we exclude from our KDE analysis the Sun-like stars that eject the meteorites, because otherwise they would influence the behaviour of the global KDE.

In the early Myr after the launch of the asteroids, the KDE highest values are confined

in the inner region of the cluster. As long as the asteroids have been ejected from the Sun-like stars, the density distribution is more broadly distributed along the cluster.

Regarding the temporal evolution of the KDE peak from the moment of the ejection of the asteroids until the end of the simulation, we can see that the highest values of the functions are in the first $1 - 2$ Myr, then the values monotonically decreases.

As expected, the resulting evolution of KDE peak of the *primordial* model has higher values with respect to the other two simulations (see Fig. 7.10), and has the same trend as the the *intermediate* one, but just scaled one order higher. The *delayed* cluster has the lower peak.

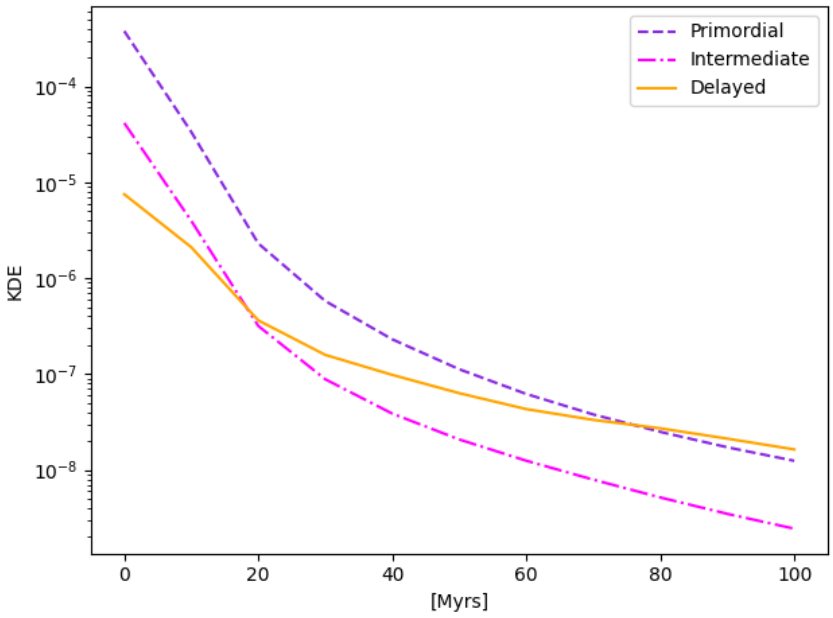

Figure 7.10: Evolution of the peak of the KDE of all the asteroids coming from the Sun-like stars. The colours and line types are the same as in Figure 7.4.

This confirms our previous theory: at the beginning of the launch, the asteroids present a higher density distribution, are close to the parental Sun-like star and to the nearby planetary systems of the cluster, so the KDE has high values.

During the subsequent stages of the asteroids dynamical evolution, the rocky bodies are more spread out, reaching the outer planetary systems but with a lower density profile. This implies that more stars can be pollutes during the evolution, but the total number of life-bearing bodies around each star decreases (and therefore we have lower values for the KDEs).

The monotonic trend in Fig. 7.10 confirms the role of the Galactic tidal field in the lithopanspermia mentioned in Sec. 7.1.5.

7.2 Bound Orbits

Even though the asteroids can be very close to the receiving planetary systems, this does necessarily mean that the bacteria cargo will land to an habitable planet. The transfer of life may require that the asteroids follow a **close orbit** around the receiving star, and then eventually land on the planets of the stellar system.

In this section, we analyse the probability that the asteroids travel along a bound orbit around the receiving star, from a single stellar point of view. More in detail, we consider the asteroids ejected from just a Sun-like star, then we compute the closest rocky neighbors of the other stellar systems and we verify if these asteroids present a bound orbit around the relative star.

The results are listed in Tab. 7.1. It is evident that the probability that the Sun-like star ejects asteroids that effectively follow a close orbit around the receiving planetary systems decreases as we launch the asteroids at later stages of the evolution of the cluster: in the *primordial* simulation 78,57% of the Sun-like stars pollute other solar systems, while in the *intermediate* model the probability decreases to 51,76%, and in the *delayed* simulation only 21,43% of the stars contribute to the lithopanspermia. This confirms the idea that the earlier the asteroids have been launched, the higher is the probability of successful transfer of microorganisms.

Moreover, 19,5% of the Sun-like stars eject asteroids that do not become bound around other planetary systems, reducing the overall chances of the pollution of the cluster.

Model	N. Sun-like stars	% N. Sun-like stars
Primordial	44/56	78,57 %
Intermediate	29/56	51,76%
Delayed	12/56	21,43%

Table 7.1: In the first column we indicate the model of the simulation, in the second one the number of Sun-like stars that launch asteroids that are subsequently bound to other planetary systems, and in the third column we have the relative percentage.

Furthermore, the total number of expected panspermia events must be reduced by the following factors, that diminish the previous probability:

- not all the asteroids are **biologically active**, therefore the number of asteroids that effectively germinate other planetary systems should be lower;
- even if the asteroids follow bound orbits, they will **not necessarily collide** with the planets of the stellar systems [1];
- the planets that eventually are polluted by the asteroids can present an **hostile environment** for the survival of the microorganisms.

[1] However, we should take into account that unbound asteroids can still collide with a planet

If we assume that only terrestrial planets are a suitable environment for life, then the number of panspermia events must be reduced by a factor of $f = 10^{-4}$ [4], therefore the favourable percentage listed in Tab.7.1 drastically decreases. Nevertheless, this should not discourage us, since the number of asteroids ejected from a Sun-like stellar system in the primordial phase of its evolution is more than 10^{16} asteroids, while we launched just 1000 because otherwise the simulation would have been prohibitively expensive from the point of view of computational resources.

7.2.1 Type of polluted stars

An additional factor that must be taken into account is the stellar type of the receiving star. We analyse the stage of the stars with the highest KDE values at a certain time in the single point of view. In particular, we can see in Fig.7.11 the percentage of receiving planetary systems per each stellar type (the relative value is reported in Tab.7.2).

It is clear that more than 50% of the stars belong to the **main sequence** (MS), providing a favourable environment to the microorganisms that come from a similar habitat (the stars responsible for the ejection of the asteroids belong to the MS too).

In addition, more than 30% of the stars with the highest KDE is instead characterized by **brown dwarfs**, that are more likely to offer a less propitious environment for the survival of the bacteria or any form of life, as seen in Sec. 2.3.1.

At the end, an important role in the lithopanspermia is played by **deeply or fully convective low-mass MS stars**, that are 10% of the total amount of most-likely receiving stars. Also in this case, the survival of the biological cargo is controversial, because it would require very specific ranges of temperature, pressure and distance of the planet from the star (see Sec.2.3.1).

Value	Stellar type
0	deeply or fully convective low mass Main Sequence stars
1	Main Sequence stars
4	core helium burning
11	carbon/oxygen white dwarf
13	neutron star
19	brown dwarf
18	planet

Table 7.2: Percentage of type of the stars with bound asteroids

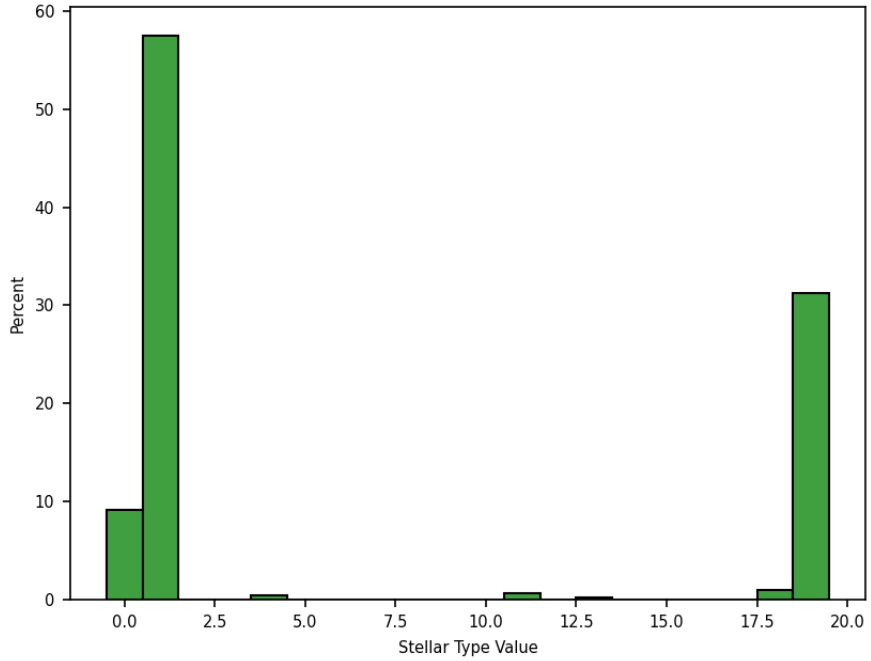

Figure 7.11: Value relative to the type of the stars with bound asteroids

Chapter 8

Conclusions

In our work we study the dynamics of life-bearing asteroids that have been ejected from an Earth-like planet in a planetary system evolving around a Sun-like star. Our hypotheses is based on the cross fertilization of other planetary systems in the same star cluster via these rocky bodies, that undergo close fly-by or a subsequent bound orbit around them (and eventually collide with the planets within systems). In particular, we perform an N-body simulation of a star cluster, modeled with a Plummer sphere with a Kroupa distribution mass function. The cluster contains around ~ 2500 stars, and among them, the Sun-like ones eject 1000 asteroids for a 100 Myr. Specifically, the ejection starts after 250 Myr from the birth of the cluster for the *primordial* simulation, after 500 Myr for the *intermediate* one, and 950 Myr in the *delayed* one.

We analyze the evolution of the biological cargo in the cluster. The results show that it is more likely that there is an effective transfer of rocks in highly crowded environments. This is the reason why in the delayed model the probability of lithopanspermia decreases, since the cluster is more dissolved due to the action of the Galactic tidal field. Thus we concluded that the earlier the asteroids have been ejected, the higher is the probability of cross fertilization in the cluster.

Moreover, most of the receiving planetary systems evolve around a Main Sequence star, therefore there is a higher chance that the bound asteroids can collide with a planet that presents favourable condition to host the terrestrial life.

In our simulation, the number of asteroids ejected from each Sun-like star is 1000, while we know from previous studies that the amount of rocky bodies ejected from a planetary system like ours is more than 10^{16}. Therefore in future works more asteroids could be implemented, in order to have a more accurate estimate of the probability of panspermia.

In conclusion, we can say that if the first forms of life were born 3.95 Gyr in the past, at the same time as the birth of the oceans, this mechanism of delivery of prebiotic substances could greatly shorten the time required for the birth and evolution of terrestrial life.

Furthermore, even if the hypothesis of the origin from space of all or part of the molecules necessary for life is not supported by certain evidence, there is no doubt that the problem of forming it in a short time could be solved if the prebiotic substances, such

as nucleic acids, amino acids and lipids, had already arrived from the outside during and after the Heavy Bombardment. It is not just a question of understanding the origin of life on this planet: if its birth is due to typical and exclusive conditions of the Earth, the exploration of the Solar System can only offer us new sterile frontiers.

Moreover, it will be necessary to look around other stars for planets similar to the Earth in size, temperature and mass that orbit around stars with the same surface temperature as the Sun. But if it depends on mechanisms that are not exclusive to our planet, then we can expect to find it also in other places, in the Solar System as around other stars other than the Sun. Solving this dilemma, for our planet, therefore means opening or closing a huge horizon [13].

Bibliography

[1]

[2] Kernel density estimation.

[3] Kernel density estimation.

[4] David N. Adams, Fred C. ; Spergel. Lithopanspermia in star-forming clusters, 2005.

[5] Kevin J Adams, Fred C ; Napier. Transfer of rocks between planetary systems: Panspermia revisited, 2022.

[6] Christine Allen and Alfredo Santillan. An improved model of the galactic mass distribution for orbit computations., 1991.

[7] James Binney and Scott Tremaine. *Galactic dynamics*. Princeton University Press, 2008.

[8] S. Chandrasekhar. Dynamical friction. i. general considerations: the coefficient of dynamical friction., 1943.

[9] Arthur N. Cox. *Allenâs Astrophysical Quantities*. Springer, 2000.

[10] M. J. ; Tout C. A. Eggleton, P. P. ; Fitchett. The distribution of visual binaries with two bright components: Erratum, 1990.

[11] Michael J. ; Tout Christopher A. Eggleton, Peter P. ; Fitchett. The distribution of visual binaries with two bright components, 1989.

[12] Rebecca elson and Piet Hut. Dynamical evolution of globular clusters, 1987.

[13] Giuseppe Galletta. *Astrobiologia, la ricerca della vita nello spazio*. Padova University Press, 2021.

[14] Ian Harry and Johannes Noller. Probing the speed of gravity with lvk, lisa, and joint observations, 2022.

[15] Gerda Horneck. Responses of bacillus subtilis spores to space environment: Results from experiments in space, 1993.

[16] Gerda Horneck. *Encyclopedia of Astrobiology*. Springer, 2011.

[17] Sverre J. Aarseth Junichiro Makino. Hermite integrator with ahmad-cohen scheme for gravitational many-body problems, 1992.

[18] Pavel Kroupa. On the variation of the initial mass function, 2001.

[19] Elizabeth A. Lada, Charles J. ; Lada. Embedded clusters in molecular clouds, 2003.

[20] Michela Mapelli. *Numerical methods for astrohpysics*. 2020.

[21] H. J. Melosh. Exchange of meteorites (and life?) between stellar systems, 2003.

[22] Yoko Funato Junichiro Makino Michiko Fujii, Masaki Iwasawa. Bridge: A direct-tree hybrid n-body algorithm for fully self-consistent simulations of star clusters and their parent galaxies, 2007.

[23] R. Miyamoto, M. ; Nagai. Three-dimensional models for the distribution of mass in galaxies., 1975.
[24] Fred C. Moorhead, Althea V. ; Adams. Giant planet migration through the action of disk torques and planet planet scattering, 2005.
[25] W. M. Napier. A mechanism for interstellar panspermia, 2004.
[26] Nobuo ; Horneck Gerda ; Melosh Henry J. ; Setlow Peter Nicholson, Wayne L. ; Munakata. Resistance of bacillus endospores to extreme terrestrial and extraterrestrial environments, 2020.
[27] Wacey David Hazen Robert M. Noffke Nora, Christian Daniel. Microbially induced sedimentary structures recording an ancient ecosystem in theca.3.48 billion-year-old dresser formation, pilbara, western australia, 2013.
[28] H. C. Plummer. On the problem of distribution in globular star clusters: (plate 8.), 1911.
[29] F. Portegies Zwart, S. F. ; Verbunt. Population synthesis of high-mass binaries., 1996.
[30] F. Portegies Zwart, S. F. ; Verbunt. Seba: Stellar and binary evolution, 2012.
[31] Stephen L. W. ; Gieles Mark Portegies Zwart, Simon F. ; McMillan. Young massive star clusters, 2010.
[32] E. ; Antoja T. ; Figueras F. Romero-Gomez, M. ; Athanassoula. Modelling the inner disc of the milky way with manifolds-i. a first step, 2011.
[33] A. van Elteren S. McMillan, S. Portegies-Zwart and A. Whitehead. Simulations of dense stellar systems with the amuse software toolkit, 2012.
[34] Mark Gieles Simon F. Portegies Zwart, Stephen L.W. McMillan. Young massive star clusters, 2010.
[35] Steve McMillan Simon Portegies Zwart. *Astrophysical Recipes, The art of AMUSE.* American Astronomical Society, 2018.
[36] Onno R. ; Eggleton Peter P. ; Han Zhanwen Tout, Christopher A. ; Pols. Zero-age main-seqence radii and luminosities as analytic functions of mass and metallicity, 1997.
[37] Steinn ; House Christopher H. Worth, R. J. ; Sigurdsson. Seeding life on the moons of the outer planets via lithopanspermia, 2013.
[38] Nishizawa Manabu ; Takahata Naoto ; Terada Kentaro ; Komiya Tsuyoshi ; Ueno Yuichiro ; Sano Yuji. Rare-earth element, lead, carbon, and nitrogen geochemistry of apatite-bearing metasediments from the $\sim$ 3.8 ga isua supracrustal belt, west greenland, 2005.
[39] Simon Portegies Zwart and Tjarda Boekholt. Numerical verification of the microscopic time reversibility of newtonâs equations of motion: Fighting exponential divergence, 2018.
[40] Simon Portegies Zwuart. The formation of solar-system analogs in young star clusters, 2019.